

# Preclinical toxicological assessment of an $\alpha$ -galactosylceramide-adjuvanted mRNA cancer vaccine in Wistar Han rats and domestic pigs

Sofie Meulewaeter,<sup>1,2</sup> Margo De Velder,<sup>1,2</sup> Diethard Reckelbus,<sup>3</sup> Kevin Mwangi,<sup>1,2</sup> Thomas Ehouarne,<sup>1,2</sup> Ilke Aernout,<sup>1,2</sup> Yanou Engelen,<sup>1,2</sup> Fellanza Halimi,<sup>3</sup> Isis Van herterycck,<sup>3</sup> Lobke De Bels,<sup>4</sup> Valerie Redant,<sup>6</sup> Louise De la Mane,<sup>6</sup> Joline Ingels,<sup>2,6</sup> Bo Coppens,<sup>6</sup> Serge Van Calenbergh,<sup>7</sup> Pieter Cornillie,<sup>4</sup> Gabriële Holtappels,<sup>8</sup> Benedicte Descamps,<sup>2,9</sup> Daisy Vanrompay,<sup>5</sup> Stefaan C. De Smedt,<sup>1,2</sup> Wim Van den Broeck,<sup>4</sup> Bart Vandekerckhove,<sup>2,6</sup> Mathias Devreese,<sup>3</sup> Rein Verbeke,<sup>1,2,10</sup> and Ine Lentacker<sup>1,2,10</sup>

<sup>1</sup>Ghent Research Group on Nanomedicines, Laboratory of General Biochemistry and Physical Pharmacy, Faculty of Pharmaceutical Sciences, Ghent University, Ottergemsesteenweg 460, 9000 Ghent, Belgium; <sup>2</sup>Cancer Research Institute Ghent (CRIG), Ghent University Hospital, Ghent University, 9000 Ghent, Belgium; <sup>3</sup>Department of Pathobiology, Pharmacology and Zoological Medicine, Faculty of Veterinary Medicine, Ghent University, Salisburylaan 133, 9820 Merelbeke, Belgium; <sup>4</sup>Department of Morphology, Imaging, Orthopedics, Rehabilitation and Nutrition, Faculty of Veterinary Medicine, Ghent University, Salisburylaan 133, 9820 Merelbeke, Belgium; <sup>5</sup>Department of Animal Sciences and Aquatic Ecology, Faculty of Bioscience Engineering, Ghent University, 9000 Ghent, Belgium; <sup>6</sup>GMP Unit CellGenTherapies, Department of Human Body Material, Ghent University Hospital, Heymanslaan 10, 9000 Ghent, Belgium; <sup>7</sup>Laboratory of Medicinal Chemistry, Department of Pharmaceutics, Ghent University, Ottergemsesteenweg 460, 9000 Ghent, Belgium; <sup>8</sup>Upper Airway Research Laboratory, Ghent University, 9000 Ghent, Belgium; <sup>9</sup>Department of Electronics and Information Systems, IbiTech-Medisip, Ghent University, 9000 Ghent, Belgium

**Galsome-NEO is a glycolipid-adjuvanted mRNA lipid nanoparticle (LNP) cancer vaccine encoding neo-epitopes for evaluation in a phase 1 study in patients with non-small cell lung cancer. To assess the safety of Galsome-NEO, a repeated-dose toxicity study was conducted in Wistar Han rats involving three intramuscular doses of 30  $\mu$ g mRNA. A dose-escalation study in piglets tested three doses of 3, 15, and 100  $\mu$ g mRNA. Rats showed a pronounced pro-inflammatory response, evidenced by cytokine secretion and an acute phase reaction. Clinical findings included temporary local reactions (maximum grade 3), elevated temperatures, and weight loss. In pigs, all doses were well tolerated. Blood analysis showed elevated alkaline phosphatase and decreased thrombocytes in rats, while pigs had reduced reticulocyte counts. Histology revealed hepatocyte vacuolation in rats and immune infiltration at injection sites in both species. In rats, blood and histology alterations resolved 3 weeks post dosing, except for immune infiltration in the connective tissue at injection sites in two females. Galsomes with mRNA encoding the *Chlamydia trachomatis* major outer membrane protein induced T cell responses in pigs. Natural killer T cell activation was observed in both species. These findings align with the safety data for the COVID-19 mRNA vaccine, Comirnaty, and demonstrate Galsomes' potential in large animals.**

## INTRODUCTION

According to Global Cancer Statistics 2020, lung cancer remains a leading cause of cancer-related deaths worldwide.<sup>1</sup> Recently, immune checkpoint inhibitors (ICIs) became the standard of care

and drastically changed the treatment landscape of lung cancer, especially non-small cell lung cancer (NSCLC). Building on the success of ICIs, numerous clinical trials are evaluating novel immunotherapies to further harness the immune system's ability to harness and destroy tumors.<sup>2</sup> Therapeutic cancer vaccines, which train the immune system to recognize and eliminate cancer cells, are showing promising results in clinical trials for NSCLC.<sup>3-5</sup> Among these, mRNA vaccines are gaining considerable interest due to their flexibility in (personalized) antigen design, rapid manufacturing, and strong potential for inducing cellular immunity. This interest is further underscored by the encouraging results from advanced clinical trials evaluating mRNA vaccines in various cancers.<sup>6-8</sup>

We previously developed a glycolipid-adjuvanted mRNA vaccine, Galsomes, which encapsulates uridine-modified (N1-methylpseudouridine, 1m $\psi$ ) mRNA encoding tumor-specific antigens in lipid nanoparticles (LNPs), composed of the ionizable lipidoid C12-200. The inclusion of the glycolipid adjuvant, alpha-galactosylceramide

Received 14 March 2025; accepted 15 May 2025;  
<https://doi.org/10.1016/j.omtm.2025.101493>.

<sup>10</sup>These authors contributed equally

**Correspondence:** Rein Verbeke, Ghent Research Group on Nanomedicines, Laboratory of General Biochemistry and Physical Pharmacy, Faculty of Pharmaceutical Sciences, Ghent University, Ottergemsesteenweg 460, 9000 Ghent, Belgium.  
**E-mail:** [rein.verbeke@ugent.be](mailto:rein.verbeke@ugent.be)

**Correspondence:** Ine Lentacker, Cancer Research Institute Ghent (CRIG), Ghent University Hospital, Ghent University, 9000 Ghent, Belgium.

**E-mail:** [ine.lentacker@ugent.be](mailto:ine.lentacker@ugent.be)



( $\alpha$ -GC), within the LNPs not only activates T cells but also engages invariant natural killer T (iNKT) cells, thereby eliciting a multifaceted anti-tumor immune response.<sup>9</sup> The administration of antigen-presenting cells loaded with  $\alpha$ -GC has been shown to be well tolerated and to extend overall survival in patients with NSCLC in phase 1/2 clinical studies.<sup>10</sup> We aim to evaluate the safety and feasibility of Galsomes encapsulating neoantigen-encoding tandem minigenic mRNA (TMG<sup>NEO</sup>),<sup>11</sup> i.e., Galsome-NEO, as monotherapy in a first-in-human phase 1a clinical study in patients with locally advanced unresectable programmed death-ligand 1-negative NSCLC.

In this study, a preclinical toxicological assessment was conducted as a critical step in advancing toward the phase 1 clinical testing of Galsome-NEO. Galsome-NEO is considered an investigational advanced therapy medicinal product, and therefore, the “*Guideline on quality, non-clinical and clinical requirements for investigational advanced therapy medicinal products (ATMPs) in clinical trials. EMA/CAT/852602/2018*” was consulted.<sup>12</sup> The intended clinical dosing regimen consists of three repeated doses with a 3-week interval, and doses will be escalated between patient cohorts.

A batch of Galsome-NEO produced according to Good Manufacturing Practice (GMP) standards was administered via intramuscular (i.m.) injection in three successive doses in two different animal models: Wistar Han rats and domestic pigs as a rodent and non-rodent animal model, respectively.<sup>13</sup> Importantly, both animals have an immune system with high similarity to the human immune system including iNKT cells reactive to  $\alpha$ -GC stimulation.<sup>14,15</sup> Additionally, the frequency of iNKT cells detected in various pig tissues is comparable to the typical frequencies found in humans.<sup>16,17</sup>

A repeated-dose study was conducted in female and male Wistar Han rats, following a similar study design for BioNTech/Pfizer’s COVID mRNA vaccine, BNT162b2 (Comirnaty), as reported by Rohde et al.<sup>18</sup> (Figure 1A). Rats received three successive doses of 30  $\mu$ g GMP-grade Galsome-NEO-formulated mRNA or an equal dose of formulation buffer as control, aligning with the intended number of clinical doses. While the EMA guideline for ATMP does not specify dose requirements, it is stated that it should offer guidance for estimating safe doses in humans.<sup>13</sup> Therefore, a total dose of 30  $\mu$ g Galsome-NEO-formulated mRNA was chosen, i.m. administered as 15  $\mu$ g doses on both hind legs. This dosage was determined by the highest volume/dose that could be administered to the hindlimb muscle of rats. Using allometric scaling, i.e., a dose conversion taking into account the body surface area which is expected to correlate with the species’ metabolism, this correlates to a human (70 kg) dose of 1,120  $\mu$ g mRNA and 3.3  $\mu$ g  $\alpha$ -GC (conversion factor 0.16).<sup>19</sup> Pigs received three doses of 3, 15, and 100  $\mu$ g of mRNA encoding the *Chlamydia trachomatis* antigen, major outer membrane protein (MOMP), corresponding to a human dose of 20, 100, and 660  $\mu$ g mRNA, respectively (conversion factor 0.95) (Figure 1B). On a daily basis, clinical symptoms were evaluated (i.e., local reactions, temperature, and body weight change). At the

day of sacrifice, blood was analyzed for biochemistry, hematology, and coagulation; a gross macroscopic evaluation was performed; vital organs were weighed; and the heart, lungs, liver, spleen, lymph node, and tissue of the injection site were collected for histological examination. As a secondary objective, iNKT cell activation, antigen-specific T cell activation, and cytokine responses were evaluated following Galsome vaccination.

## RESULTS

### Clinical observations

The clinical health status of rats in the clinical cohort was monitored after each vaccination by measuring body weight and temperature as well as evaluating local reactions (Figure 2A) using the Draize scoring system (Figures S1 and S2). Significant changes were observed in rats treated with Galsome-NEO compared to control rats, injected with 9% sucrose TRIS, across all parameters. These changes were most pronounced 24 h after injection; thus, parameters are presented at the 24-h mark after each dose (Figures 2B–2D). Local reactions (Figure 2B) primarily appeared as erythema with less frequent occurrences of edema. The severity did not exceed grade 3, with most reactions classified as grade 1 and 2. These local reactions were more prominent in female rats and tended to occur more frequently after the second and third dose. In most cases, the rats recovered from the local side effects within a few days (Figure 2E). Body temperature showed significant elevation compared to control rats, ranging from +1.2°C in male and female rats after the first dose to +2.5°C in female rats after the second and third dose. This suggests a contribution of both sex and the number of doses to reactogenicity (Figure 2C). After 48 h, body temperature returned to levels similar to those of control rats (data not shown). Galsome-NEO-treated rats also experienced considerably more weight loss compared to control rats. On average, weight loss was 8.5% after the second dose and remained below or equal to 10%, except for one male rat that lost 13% (Figure 2D). Since rats returned to their original initial weight 120 h post injection (Figure 2F), we attribute the weight loss to the rats temporarily experiencing malaise due to treatment. Once again, reactions to the second and third dose were more pronounced compared to the first dose.

The clinical health of piglets in response to vaccination is shown in Figure 3. Edema was not observed in either the vaccinated or control groups, and only some grade 1 erythema was noted 24 h post injection. However, this occurred equally or more frequently in the control group and was therefore not considered Galsome-related for any of the doses (Figure 3B). Furthermore, no local reactions were observed at later time points (Figure 3E).

No significant elevations in body temperature (Figure 3C) or changes in body weight (Figure 3D) were observed when comparing Galsome-MOMP piglets to control piglets. However, it should be noted that all animals experienced a temporary drop in weight post injection, which was slightly more pronounced in male Galsome-MOMP piglets after the 15 and 100  $\mu$ g doses (Figures 3D and 3F). Slight increases in body temperature were also recorded

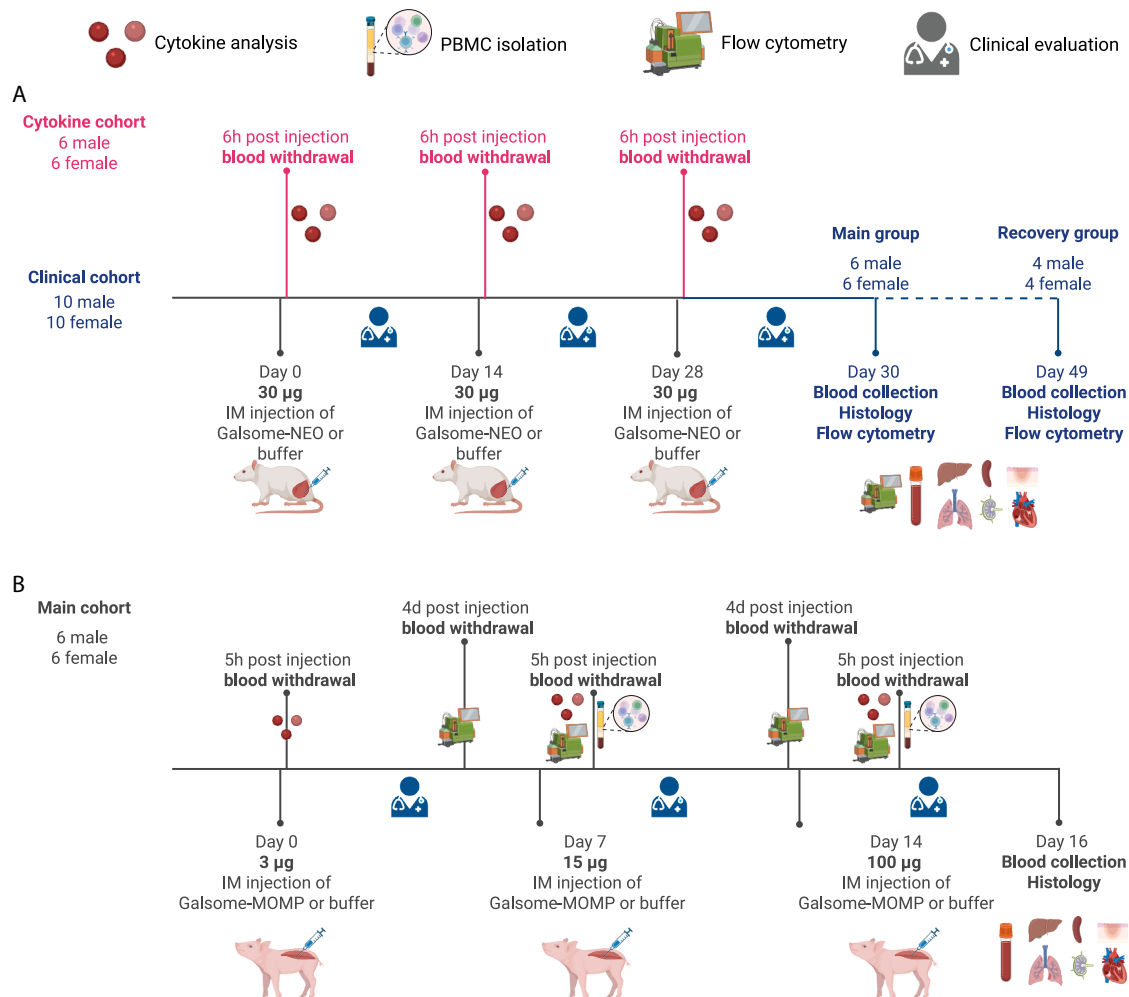


**Figure 1. Study design of preclinical toxicity studies performed in Wistar Han Rats and domestic piglets**

Schematic overview of the dosing regimen and days of sacrifice for the repeated-dose study in Wistar Han rats (A) and dose-escalation study in domestic piglets (B). In a separate study, 1 male and 1 female piglet (5 weeks) received a single dose i.m. of 100 µg MOMP-encoding mRNA packaged in Galsomes. Blood was collected in heparin tubes 7 days after injection, and PBMCs were isolated and restimulated with MOMP peptide to assess MOMP-specific T cell proliferation. Created with [Biorender.com](#).

in Galsome-MOMP piglets compared to controls after the 15 and 100 µg doses, particularly in female piglets.

### Cytokine secretion and inflammatory response

To assess the inflammatory responses to repeated administration of Galsomes in rats and pigs, the concentrations of chemokines (chemokine [C-X-C motif] ligand 1 [CXCL1], monocyte chemoattractant protein-1 [MCP-1], and interleukin [IL]-8) and cytokines (IL-1, IL-6, IL-17, IL-18, TNF-α, IL-12, interferon [IFN]-γ, IL-4, IL-10, IL-33, IFN-α, and granulocyte-macrophage colony stimulating factor [GM-CSF]) were measured in piglets, rats, or both species. A separate cohort of rats, referred to as the cytokine cohort, was used for this purpose, and plasma was collected 6 h after each injection (Figure 4A). In pigs, serum was collected 5 h post injection from animals involved in the main study (Figure 4F). In Galsome-NEO-

treated rats, elevated levels of MCP-1, IL-6, and CXCL1 were observed after each dose (Figures 4B–4D). Additionally, there was a trend toward increased IFN-γ concentrations after the second and third vaccine dose, although this was not statistically significant (Figure 4E). Other measured cytokines (tumor necrosis factor alpha [TNF-α], IL-10, GM-CSF, IL-18, IL-12p70, IL-1β, IL-17A, IL-33, and IL-1α) were not increased (Figure S3). In piglets, a notable elevation of IL-6 ( $p = 0.06$ ) was observed after the third dose of 100 µg Galsome-MOMP. Other measured cytokines, including IFN-α, IFN-γ, IL-1β, IL-10, IL-12/IL-23p40, IL-4, IL-8, and TNF-α, did not show significant changes (Figure S4).

### Blood biochemistry, hematology, and coagulation parameters

Blood was collected 48 h after the final dose of either Galsomes or buffer (control group) and analyzed for blood biochemistry,

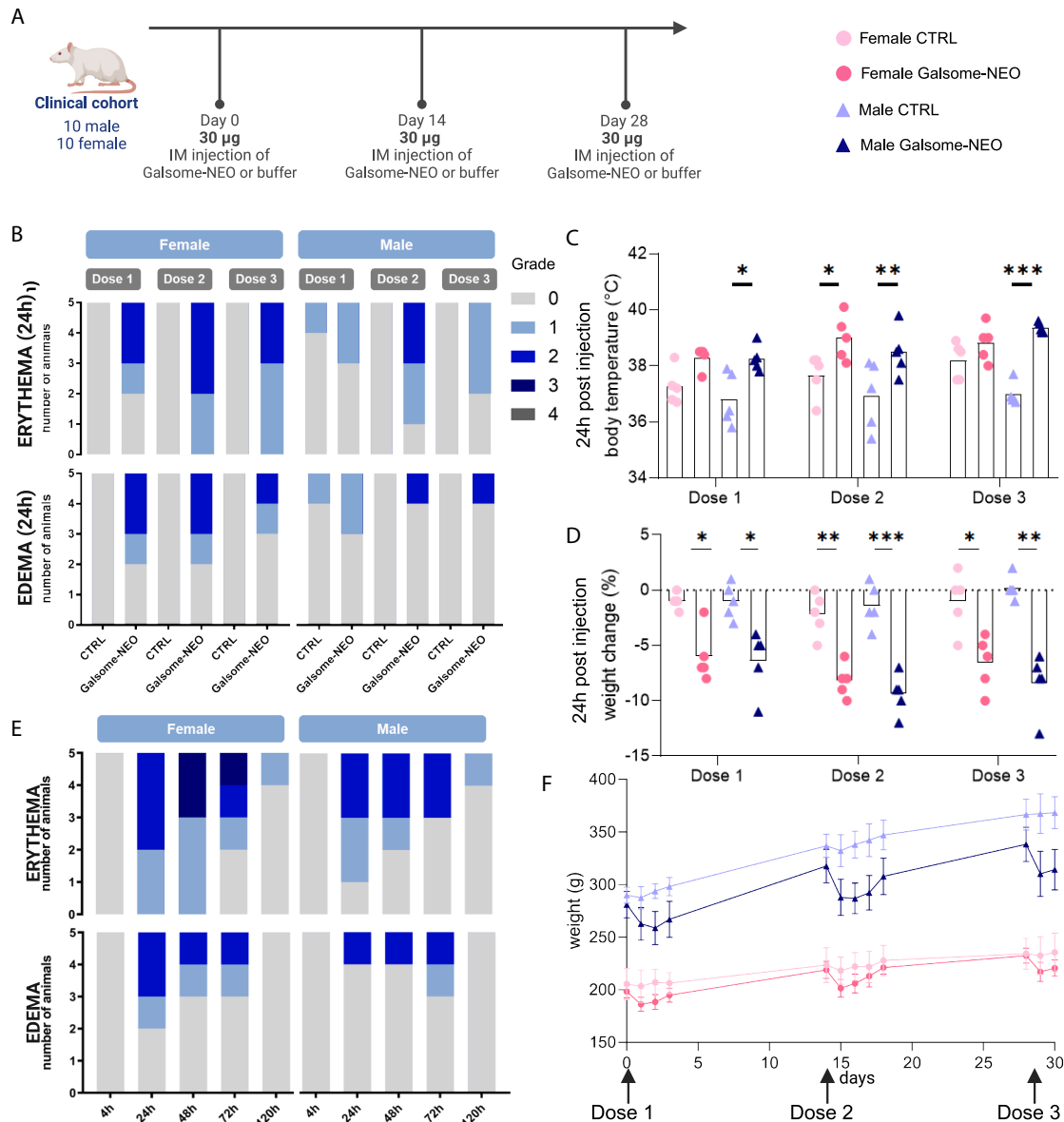


**Figure 2. Clinical evaluation of Wistar Han rats vaccinated with three repeated doses of 30 µg Galsome-NEO**

(A) Ten male and 10 female 10-week-old Wistar Han rats were randomly allocated to the clinical cohort and received intramuscularly (i.m.) in the biceps femoris three repeated doses of either 30 µg patient neo-epitope mRNA encapsulated in Galsomes (Galsome-NEO rats) or an equal volume of 9% sucrose Tris 20 mM buffer (CTRL rats). The total dose was divided over both hind legs. (B–D) Clinical parameters in male and female rats 24 h after i.m. injection with buffer (CTRL) or 30 µg Galsome-NEO. (B) Local reactions (erythema and edema) were evaluated using the Draize scoring system and received a grade 0–4 depending on the severity of the local reactions. Both injection sites were evaluated, and the highest score obtained for each rat is shown in the graph. (C) Rectal temperature 24 h post injection. (D) Body weight change (%) 24 h after injection relative to the weight of the same animal 0 h after injection. (C and D) Symbols represent individual data points and mean is indicated by a bar, statistical analyses on datasets were performed by using two-way ANOVA ( $*p < 0.05$ ,  $**p < 0.01$ ,  $***p < 0.001$ ). (E) Local reactions (erythema and edema) in male and female rats 4, 24, 48, 72, and 120 h after i.m. injection with Galsome-NEO. (F) Absolute daily body weights (g) of male and female rats treated with 9% sucrose Tris 20 mM buffer (CTRL) or Galsome-NEO (mean  $\pm$  SD). Images created with [Biorender.com](#).

hematology, and coagulation parameters to evaluate any systemic toxicity of Galsome-NEO or Galsome-MOMP in rats (main group) and piglets, respectively. In the rat recovery group, blood was analyzed 3 weeks after the last dose to assess whether any changes

observed in the main group were reversible, indicating sub-chronic toxicity of Galsome-NEO. The results of the blood analysis are presented in [Table S1](#) for rats and [Table S2](#) for piglets with significantly altered parameters highlighted in bold.

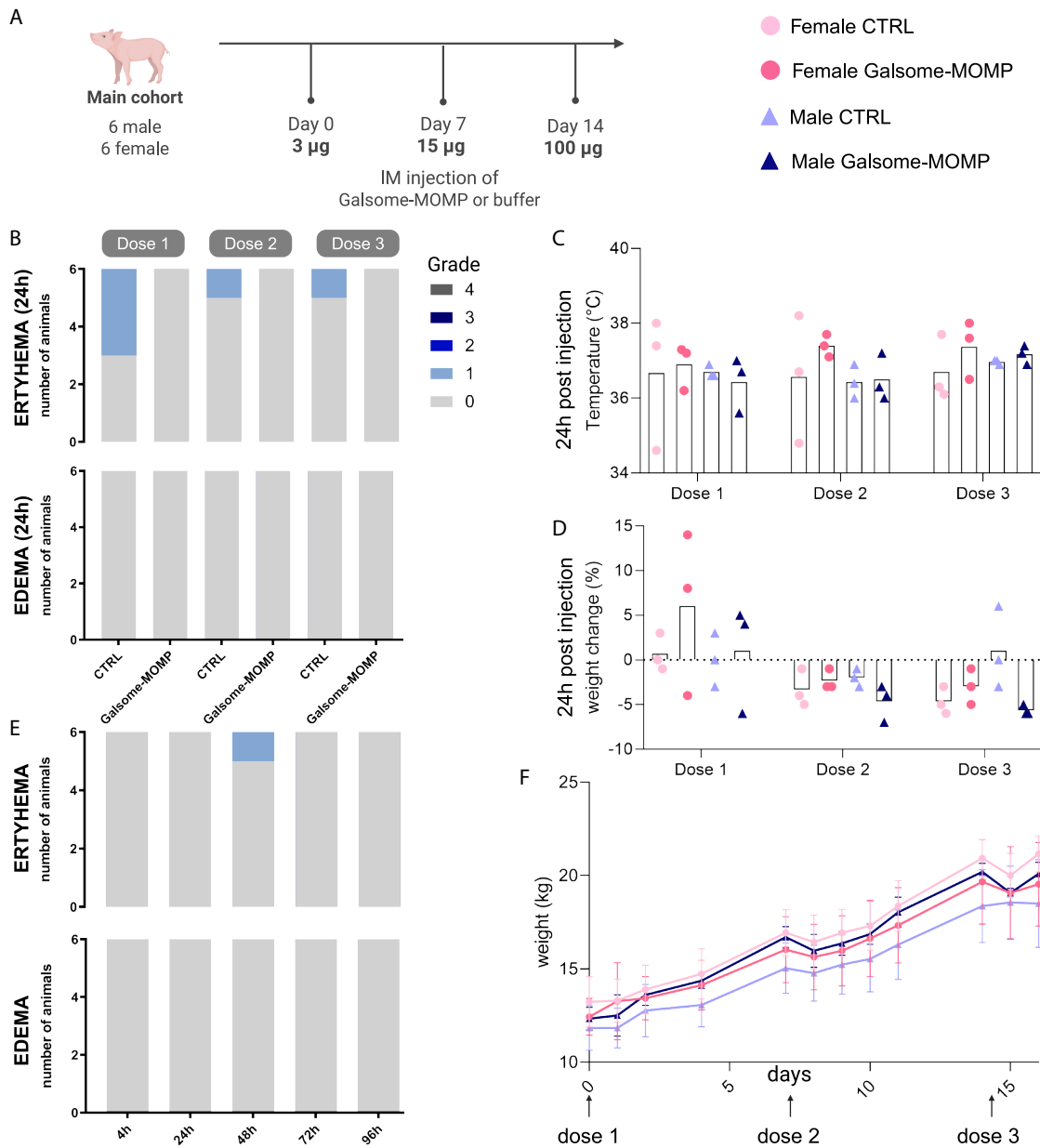


**Figure 3. Clinical evaluation of domestic piglets vaccinated with three increasing doses of Galsome-MOMP**

(A) Six male and 6 female 7-week-old piglets received intramuscularly (i.m.) in the left dorsal longitudinal muscle increasing doses of 3, 15, or 100 µg *C. trachomatis* major outer membrane protein (MOMP) encoding mRNA encapsulated in Galsomes (Galsome-MOMP piglets) or an equal volume of 9% sucrose Tris 20 mM buffer (CTRL piglets). (B–D) Clinical parameters in male and female piglets 24 h after i.m. injection with buffer (CTRL) or increasing doses of Galsome-MOMP. (B) Local reactions (erythema and edema) were evaluated using the Draize scoring system and received a grade 0–4 depending on the severity of the local reactions. (C) Body temperature is measured by scanning a subcutaneously implanted thermal microchip. (D) Body weight change (%) 24 h after injection relative to the weight of the same animal 0 h after injection. (C and D) Individual data are shown and bars indicate mean value, statistical analyses on datasets were performed by using two-way ANOVA but did not detect any significance. (E) Local reactions at the injection site in piglets 4, 24, 48, 72, and 96 h after i.m. injection with Galsome-MOMP. (F) Absolute daily body weights (kg) of individual male and female piglets (individual data points) treated with 9% sucrose Tris 20 mM buffer (CTRL) or Galsome-MOMP, full line represents mean weights. Images created with [Biorender.com](https://www.biorender.com).

Hematological findings in rats indicated signs of acute inflammation, with increased leukocyte counts, most notably for monocytes (2.6-fold) and neutrophils (3.7-fold). Leukocyte counts in the recovery

group returned to normal, comparable to the levels measured in control rats. 48 h after the last treatment with 100 µg of Galsomes, no elevated leukocyte counts were measured in pigs.

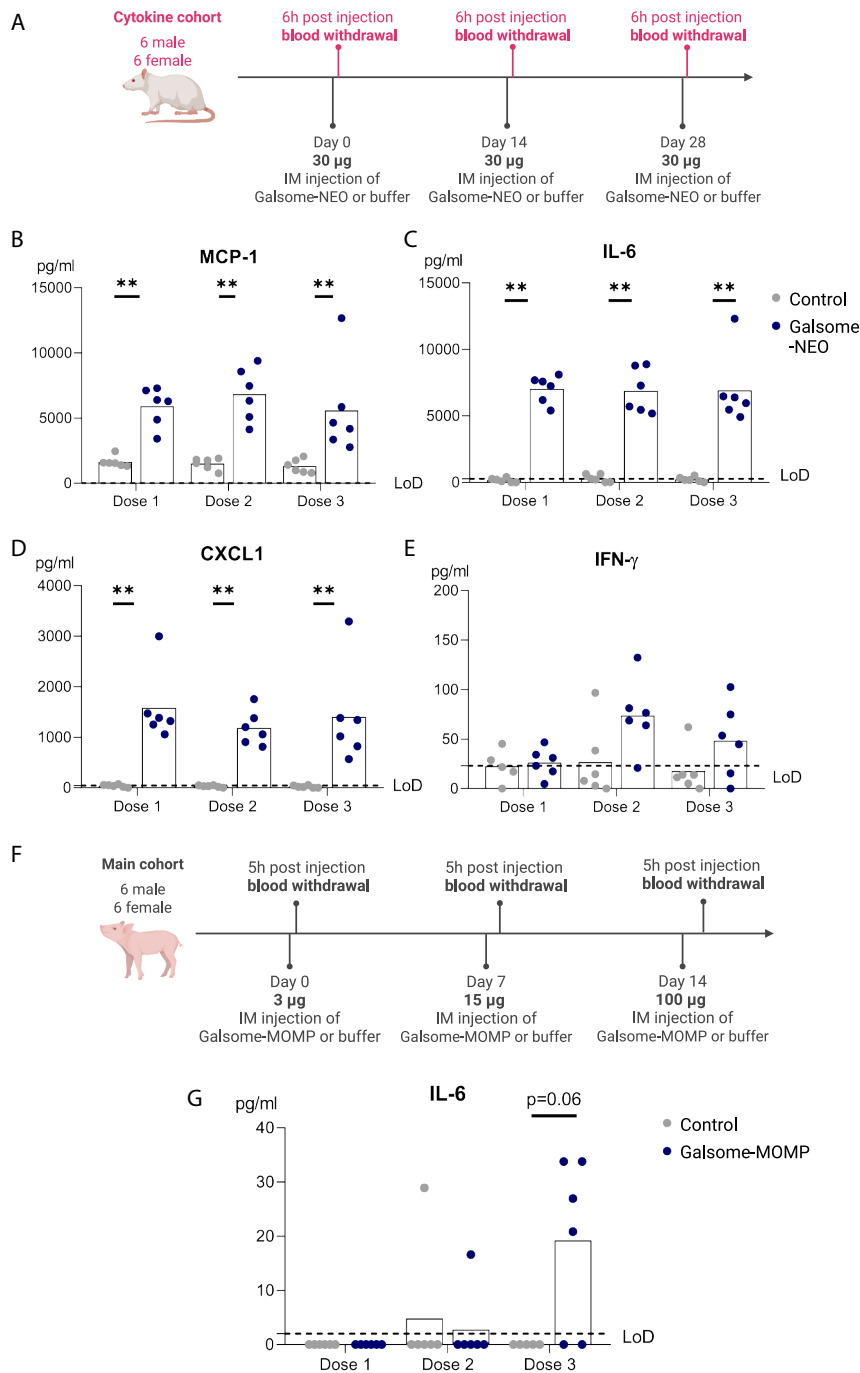


**Figure 4. Cytokine response in rats and pigs**

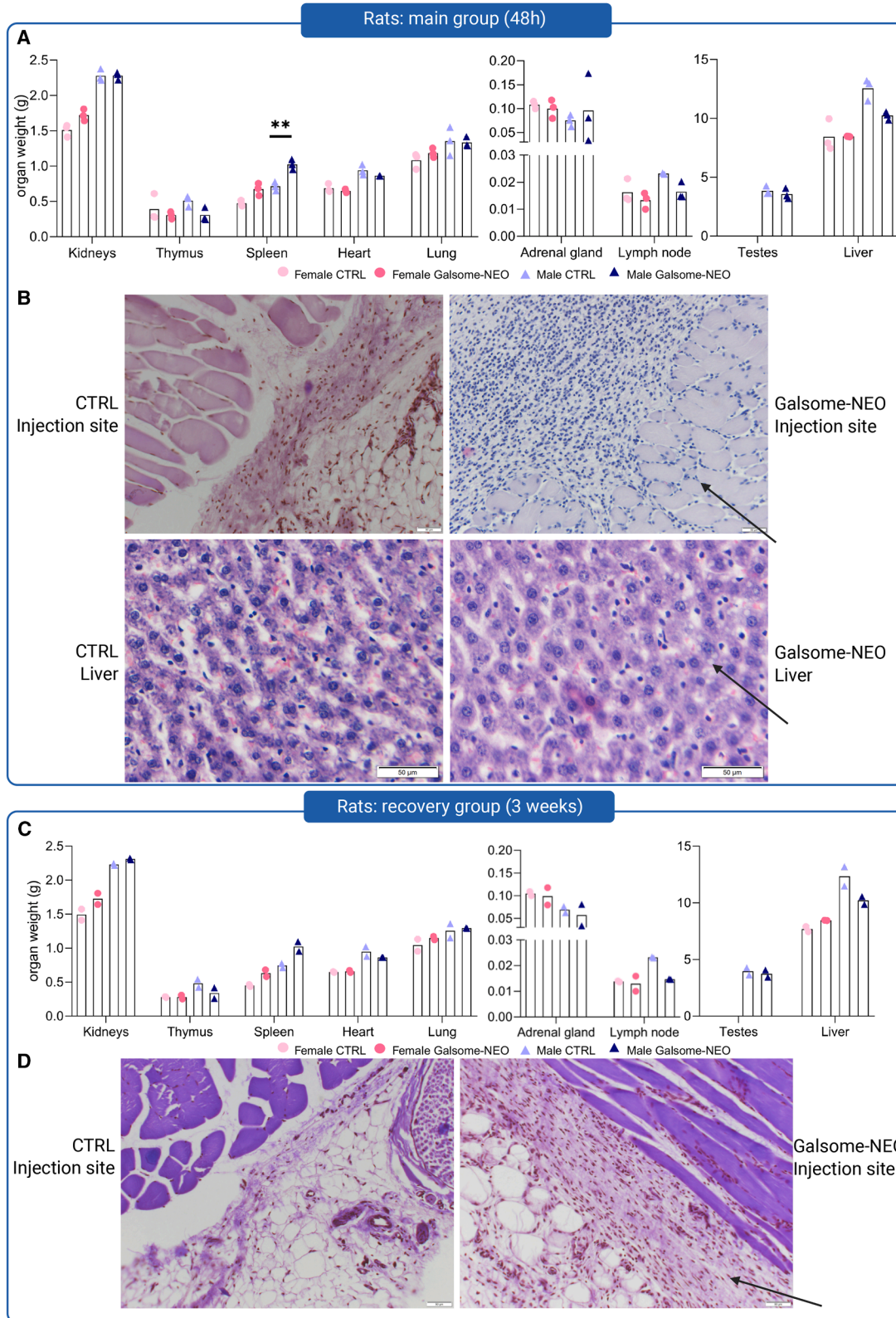
(A) A separate cytokine cohort of 6 male and 6 female rats was included in the study to evaluate cytokine secretion in rats shortly (6 h) after injection. The rats received an i.m. injection of either 30 µg of patient neo-epitope mRNA encapsulated in Galsomes (Galsome-NEO) or an equal volume of 9% sucrose Tris 20 mM buffer (control). (B–E) Plasma cytokines (TNF-α, IL-10, IFN-γ, CXCL1, MCP-1, GM-CSF, IL-18, IL-12p70, IL-1β, IL-17A, IL-33, IL-1α, and IL-6) were measured using a LEGENDplex assay. Elevated cytokine levels after NEO-Galsome injection are shown for CXCL1 (B), IL-6 (C), MCP-1 (D), and IFN-γ (E). (F) In pigs, blood was collected from the main cohort (6 male and 6 female pigs) shortly (5 h) after injection. The piglets received an i.m. injection of 3, 15, or 100 µg MOMP mRNA encapsulated in Galsomes (Galsome) or an equal volume of 9% sucrose Tris 20 mM buffer (control). (G) Serum cytokines (IFN-α, IFN-γ, IL-1β, IL-10, IL-12/IL-23p40, IL-4, IL-6, IL-8, and TNF-α) were measured using a ProcartaPlex assay. Among these, only IL-6 showed a notable elevation ( $p = 0.06$ ). Individual data points and means are shown. Statistical analyses on datasets were performed using the Mann-Whitney test, and data points below the limit of detection (LoD) were set at the LoD value for analysis ( $*p < 0.05$ ,  $**p < 0.01$ ,  $***p < 0.001$ ). Images created with [Biorender.com](https://www.biorender.com).

elevated in male (800-fold) compared to females (200-fold). A reduction was also detected in albumin concentration, a negative acute phase protein, in serum of rats treated with Galsome-NEO. However, no changes in albumin levels were observed in pigs, which is consistent with previous findings that albumin levels remain stable in pigs during infection,<sup>20,21</sup> suggesting that it may not be a sensitive marker of inflammation in this species.

Both rats and pigs vaccinated with Galsomes showed a decrease in reticulocytes (immature red blood cells) by 13% and 35%, respectively, with the latter being significant. However, no anemia developed at 3 weeks, indicating only a temporary inhibition of erythropoiesis. In Galsome-NEO-treated rats, platelet counts were significantly reduced by 32%, 48 h after the final dose but returned to normal 3 weeks after the final dose. Additionally, prolonged

intrinsic coagulation pathways were observed as prothrombin time was elevated by 16%. Fibrinogen levels were only slightly reduced indicating limited activation of the clotting cascade. However, fibrinogen levels at 3 weeks appeared artificially low, likely due to clot activation during blood draw. In piglets, thrombocyte counts remained unchanged with no significant alterations in clotting times or fibrinogen levels.

Consistent with these findings, we detected significantly elevated levels of acute phase proteins in the serum of rats, including alpha-1 acid glycoprotein (A1AGP, 40-fold) and alpha-2 macroglobulin (A2M, 428-fold). In piglets, acute phase proteins were elevated to a lesser extent, with C-reactive protein (CRP) increasing 2.4-fold, 48 h after Galsome vaccination. A1AGP levels were similarly upregulated in male and female rats, but A2M was much more



(legend on next page)

No obvious toxicity was observed in red blood cells (lactate dehydrogenases) kidneys (creatinine), heart (creatinine kinase), and liver (alanine aminotransferase [ALT] and aspartate aminotransferase [AST]) in either rats or pigs. However, in rat serum, notable changes were observed 48 h after the last Galsome-NEO dose with levels of alkaline phosphatase (AP) elevated by 66%. This increase normalized 3 weeks after vaccination potentially due to transient gall duct obstruction or altered bone metabolism. In piglets, AP levels were comparable between control and Galsome-MOMP groups. AST, an enzyme found in the liver, but also present in other tissues such as the heart, muscles, and kidneys, remained unchanged. Serum cholesterol levels decreased by 34% in pigs and by 25% in rats, 48 h after the last Galsome dose compared to control groups. Triglycerides levels were also significantly decreased in rats. These reductions in cholesterol and triglycerides were likely due to transient anorexia during the inflammatory period and normalized 3 weeks after the final dose.

#### Postmortem organ evaluation

Organs were collected after blood sampling and euthanasia, either 48 h after the final injection (main group) or 3 weeks after the final injection (recovery group) in rats. A gross macroscopic evaluation was performed, and selected organs were weighted and histologically examined. Apart from the injection site, no significant macroscopic changes were observed. At the injection site, a small fibrinous layer covering the muscle was noted. The organs (lungs, heart, liver, spleen, inguinal lymph node, kidneys, adrenal gland, and testes) were weighed, and a significant increase in the weight of the spleen was observed in male Galsome-treated rats of the main group (Figure 5A), which returned to normal in the recovery group (Figure 5C). We did not notice any changes in weight of other organs of vaccinated rats from either the main or recovery group. In piglets, no significant changes in organ weights were found 48 h after the final dose (Figure 6A).

Hematoxylin and eosin (H&E) staining of tissue sections from the spleen, lungs, heart, liver, inguinal lymph node, and injection site was analyzed by a pathologist in a blinded manner. Alterations were observed at the injection site and liver of Galsome-treated rats in the main study group (Figure 5B). Specifically, immune cells were abundantly present between and around muscle cells at the injection site of Galsome rats. This inflammation largely subsided in the recovery group, although a relatively high number of immune cells remained in the connective tissue surrounding the muscle in two female rats from the recovery group, indicating some persistent

inflammatory response at the injection site (Figure 5D). Liver tissue sections from Galsome-treated rats in the main study group showed vacuoles in hepatocytes, which were absent in control rats (Figure 5B). There was no histological evidence of hepatic tissue damage, and this observation was reversible, as no vacuoles were detected in the liver of Galsome-treated rats from the recovery group. Similar to the rats, inflammation was also observed at the injection site in piglets, though less pronounced (Figure 6B). In piglet liver tissue, we could not observe any clearly aligned vacuoles; however, in some cases, we observed signs of vacuolization as indicated by more transparent regions in the liver. Due to the random occurrence of this observation of vacuolization, we do not attribute this to Galsome treatment but rather consider this as an artifact due to less optimal fixation in certain samples.

#### Immune responses: iNKT cells and T cells

As a secondary objective, we assessed the potential of Galsomes to elicit iNKT cell and antigen-specific T cell responses. Evaluating antigen-specific T cell responses in rats was not possible as they received patient-specific neo-epitope-encoding mRNA, which is selectively presented by human leukocyte antigen-A2.<sup>11</sup> However, by utilizing mRNA encoding the *C. trachomatis* antigen, MOMP, we were able to monitor T cell responses in the piglet study.<sup>22</sup>

In both species, iNKT cells have been reported and shown to react to  $\alpha$ -GC stimulation.<sup>14,15</sup> To analyze iNKT cell proliferation in rats, spleen and inguinal lymph nodes were isolated 48 h (main group) and 3 weeks after the final dose (recovery group) (Figure 7A) and stained for iNKT cell markers (CD161 and CD3) (Figure 7B). Flow cytometry analysis revealed a slightly higher number of iNKT cells in the inguinal lymph node of Galsome-treated rats compared to control rats, both 48 h and 3 weeks after the final dose (Figure 7C). In contrast, there was a trend toward lower iNKT cell frequencies in the spleen (Figure 7D). In addition, we also evaluated natural killer (NK) cells (CD161<sup>+</sup> CD3<sup>-</sup>) as iNKT activation can induce downstream NK cell activation. However, we did not observe elevated numbers of NK cells in the inguinal lymph node after Galsome vaccination (Figure S5).

iNKT responses in piglets were studied in blood samples collected 4 and 7 days after the first and second doses (Figure 7E). Whole blood was stained for flow cytometry detection of iNKT cells by using an anti-CD3 antibody and mouse CD1d PBS-57 tetramer, with an unloaded tetramer included as control (Figure 7F). Mouse CD1d PBS-57 tetramers have previously been shown to cross-react with

**Figure 5. Postmortem organ evaluation 48 h and 3 weeks after the final dose in rats reveals morphological alterations in the liver and at the injection site** (A and C) Absolute organ weights (g) of kidneys, thymus, testes, spleen, heart, lung, liver, adrenal gland, and lymph node of rats in the main group ( $n = 6$ ) and recovery group ( $n = 4$ ). Organs were excised and weighed 48 h (A) or 3 weeks (C) after the last dose of a series of three repeated doses from rats of the main group and recovery group, respectively. Symbols represent individual data points ( $n = 3/2$ ) and mean values are shown. Multiple unpaired t test was performed without correction ( $*p < 0.05$ ,  $**p < 0.01$ ,  $***p < 0.001$ ). (B) Representative images of H&E-stained liver tissue sections and tissue from the injection site from rats of the main group. Inflammatory cells located between and around muscle cells of Galsome-NEO-treated rats are indicated by arrows. Liver tissue sections show vacuoles in hepatocytes (indicated by arrows) of Galsome-NEO-treated rats. (D) H&E-stained tissue sections from the injection site 3 weeks after the final injection (recovery group) show macrophages (indicated by arrows) in the connective tissue surrounding muscle cells of female Galsome-NEO-treated rats.

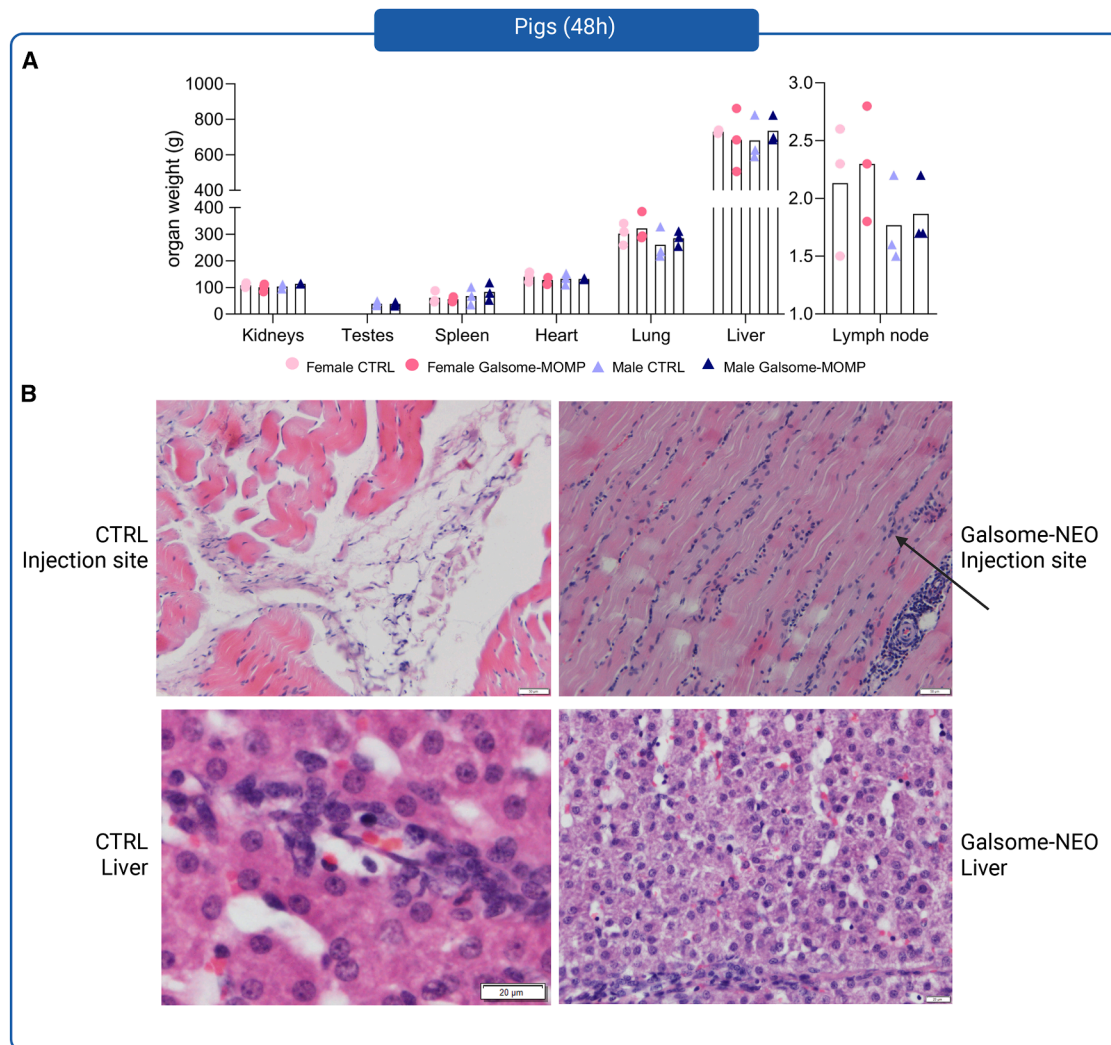


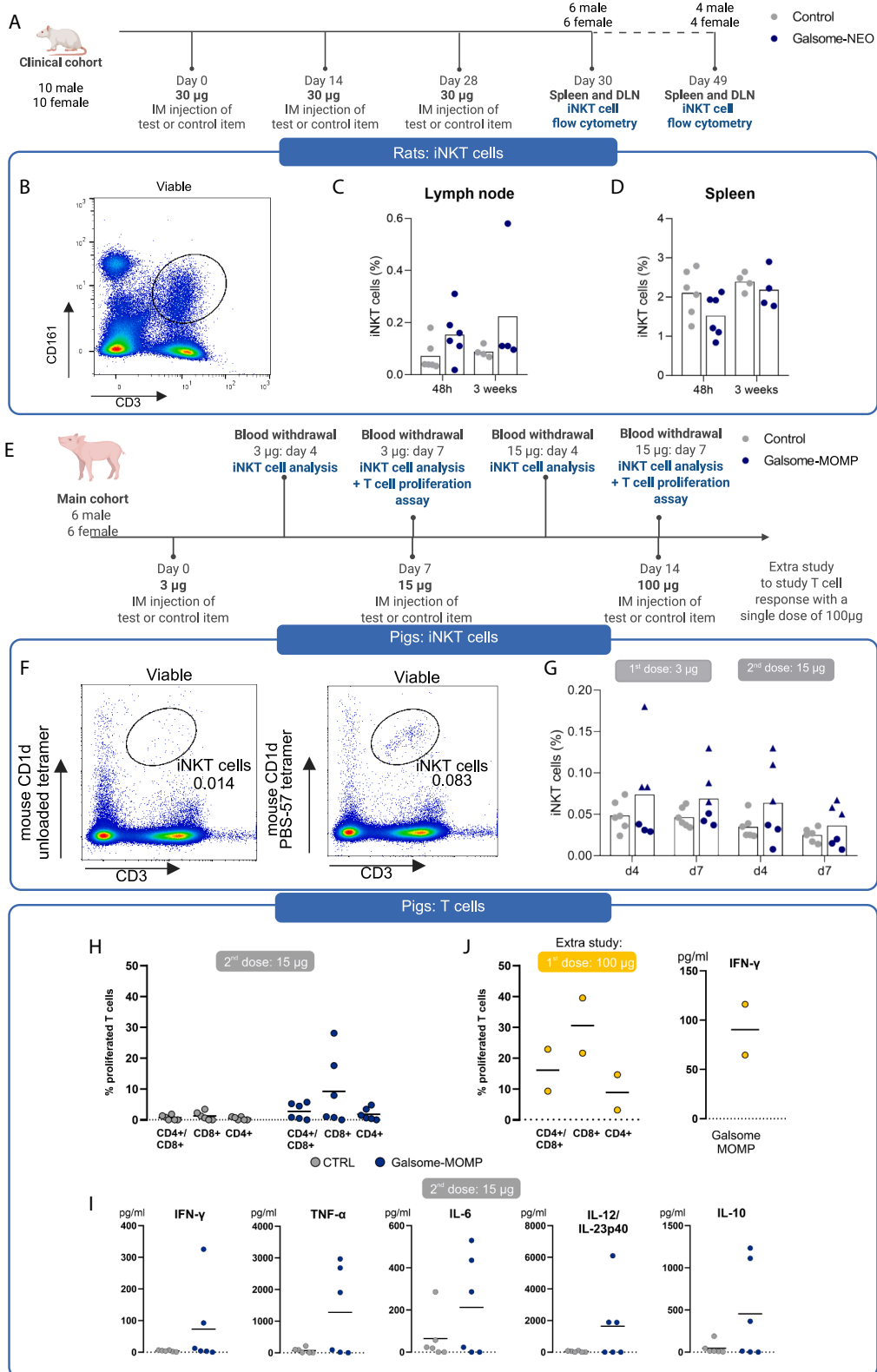
**Figure 6. Organ weights of selected organs in pigs 48 h after the final dose**

(A) Absolute organ weights (g) of kidneys, testes, spleen, heart, lung, liver, and lymph node of piglets (6 females and 6 males). Organs were excised and weighed 48 h after the final dose of repeated injections of Galsome-MOMP or buffer (control). Symbols represent individual data points ( $n = 3$ ) with mean values shown. Multiple unpaired *t* test was performed without correction and no significant differences were found. (B) Representative images of H&E-stained sections of liver tissue and tissue from the injection site in pigs 48 h after the final dose. Inflammatory cells located between muscle cells and around muscle cells of Galsome-MOMP-treated pigs are indicated by arrows. No clear vacuoles were observed in the liver tissue of pigs.

porcine iNKT cells.<sup>23,24</sup> Increased levels of iNKT cells in the blood of piglets were observed following the first and second doses of Galsomes, in 3 of the 6 vaccinated piglets that consistently responded to the treatment (indicated by triangles) (Figure 7G).

To detect T cell responses, peripheral blood mononuclear cells (PBMCs) were isolated from whole blood collected 7 days after the first and second Galsome-MOMP dose and pulsed with a 25-amino-acid (aa)-long peptide containing CD4<sup>+</sup> and CD8<sup>+</sup> T cell epitopes, derived from the MOMP antigen. CellTrace Violet staining was used to quantify T cell proliferation after peptide pulsing. We observed increased T cell proliferation of CD8<sup>+</sup>, CD4<sup>+</sup>, and CD8/

CD4 double-positive cells in three out of six Galsome-treated animals (Figure 7H). These results were corroborated by cytokine analysis in the supernatant of peptide-pulsed PBMCs from vaccinated animals, showing elevated production of IFN- $\gamma$ , TNF- $\alpha$ , IL-6, IL-12/IL-23p40, and IL-10 (Figure 7I). It should be noted that we could not evaluate the T cell response after the last final dose of 100  $\mu$ g, since we had to euthanize the animals at 48 h post injection for acute toxicity evaluation. Instead, an extra experiment was conducted with two piglets (1 female/1 male) that both received a single dose of 100  $\mu$ g MOMP-encoding mRNA encapsulated in Galsomes, showing robust T cell proliferation and IFN- $\gamma$  production at this higher dose (Figure 7).



(legend on next page)

## DISCUSSION

In this study, we evaluated the preclinical toxicity of Galsome-NEO, a glycolipid-adjuvanted mRNA LNP containing the ionizable lipid C12-200, intended for use as a therapeutic cancer vaccine in a phase 1 clinical study in patients with NSCLC. The study was conducted in two animal species: Wistar Han rats and domestic piglets (*Sus scrofa*). Three doses of GMP-grade Galsome-NEO were i.m. administered to assess toxicity. Toxicity in both species was assessed by evaluating local tolerance, clinical parameters, and blood analysis (biochemistry, hematology, coagulation, and cytokine levels) and conducting a postmortem organ evaluation (macroscopic observation and histology). As a secondary objective, immune responses were analyzed by measuring antigen-specific T cell responses and iNKT cell responses, which are primary targets of the Galsome vaccine.

Rats displayed pronounced clinical symptoms including erythema, edema, elevated body temperatures, and weight loss, following each Galsome-NEO dose (30 µg). Local reactions were limited to grade 3, and weight loss did not exceed the 10% limit suggested for defining the maximum tolerated dose in rats.<sup>25</sup> All clinical symptoms resolved within a few days. No notable clinical symptoms were observed in pigs, especially in response to the lower doses of 3 and 15 µg. The clinical observations in rats were in line with the strong upregulation of cytokines IL-6, MCP-1, and CXCL1 in these animals shortly (6 h) after injection. IL-6 is known to act as an endogenous pyrogen inducing fever, which corresponds with the elevated temperatures observed in rats.<sup>26</sup> Note that IL-6 was also slightly upregulated in pigs after receiving the highest final dose of 100 µg. The elevated IL-6 levels are consistent with findings in other studies where mRNA LNPs<sup>27,28</sup> and even empty LNP induced IL-6 and contributed to the adjuvant effect of LNP carriers in eliciting antibody responses.<sup>29</sup> Consistent with elevated IL-6 cytokine levels,<sup>30</sup> both pigs and rats showed significant increases in circulating acute phase proteins 48 h after the final dose, indicating acute inflammation in both species. In pigs, CRP elevation (2-fold increase) was relatively modest. In contrast, in rats, the levels of A1AGP (40-fold increase) and A2M (428-fold increase) were in line with what was

reported for BNT162b2.<sup>18</sup> These acute phase responses correlate with the observed clinical symptoms of malaise and local inflammation (erythema and edema), which were temporary and did not exceed grade 3 in severity.

Besides cytokines and acute phase proteins, chemokines were also elevated in rats. Specifically, MCP-1 and CXCL1 were increased. MCP-1 is involved in recruiting monocytes while CXCL1 recruits neutrophils. The elevated levels of these chemokines could be linked to the immune cell influx observed in the histological sections of the injection site. Neutrophil influx at the injection site was previously observed upon mRNA LNP injection.<sup>28</sup> While MCP-1 is commonly induced by muscle injury, other cytokines typically associated with inflammation and muscle injury in humans such as TNF-α and IL-1β were not detected.<sup>31</sup>

The early clinical symptoms and elevated cytokines are indicative of an innate immune response to the Galsome formulation. Recent studies emphasize the pivotal role of LNPs in mediating inflammatory immune responses and highlight the importance of ionizable lipids in this process.<sup>27–29</sup> In line with previous observations,<sup>32,33</sup> our study also demonstrated that the type of ionizable lipid incorporated in the Galsome formulation impacts proinflammatory cytokine secretion, with the C12-200 ionizable lipid inducing higher cytokine secretion than the SM-102 ionizable lipid.<sup>34</sup> Although mRNA encapsulated in the Galsome formulation contains 1mψ modifications and Cap 1 to minimize innate immune activity, it cannot be excluded that mRNA or potential byproducts (e.g., double-stranded RNA) are also sensed by immune cells.<sup>35</sup> Notably, we did not measure IFN-α in pigs (IFN-α was not included in the rat cytokine panel).

Histological examination in the rat study revealed morphological alterations not only in tissue collected from the injection site but also liver tissue, characterized by the presence of vacuoles in hepatocytes but without signs of hepatic tissue damage. Similar findings were also reported in preclinical rat toxicity studies evaluating both BNT162b2 and mRNA-1273 (COVID mRNA vaccines).<sup>36,37</sup> In a report on the repeated-dose toxicity study of BNT162b2 in Wistar Han rats, Pfizer

### Figure 7. Immune responses to Galsome vaccination in rats and piglets

(A) Wistar Han rats in the clinical cohort were sacrificed 48 h (main group) or 3 weeks (recovery group) after the final injection of three successive injections of either 30 µg Galsome-NEO (Galsome-NEO) or buffer (control). Spleen and inguinal lymph node were isolated and processed for flow cytometry analysis of iNKT cells. (B) Gating strategy for identifying iNKT cells in rats. Viable cells positive for CD161 (NK1.1 receptor) and CD3 were classified as iNKT cells (CD161<sup>+</sup>/CD3<sup>+</sup>). Fraction of iNKT cells within the viable cell population in the (C) spleen and (D) lymph node of control animals (3 doses of buffer) and Galsome-NEO (3 doses of 30 µg TMG<sup>NEO</sup> mRNA Galsomes) 48 h ( $n = 6$ ) and 3 weeks ( $n = 4$ ) after the final dose. (E) Heparinized blood was drawn from piglets (6 females/6 males) 4 and 7 days after the first and second dose of buffer (control) or MOMP-encoding mRNA packed in Galsomes (Galsome-MOMP). The first dose contained 3 µg mRNA and the second dose 15 µg mRNA. (F) Four and 7 days after the first and second injection, whole blood was stained to detect iNKT cells. The gating strategy is shown, with cells positive for CD3 and mouse CD1d PBS-57 tetramer identified as iNKT cells. An unloaded CD1d tetramer was included as a control to ensure specific binding. (G) Fraction of iNKT cells within the viable cell population in the blood of piglets 4 and 7 days after the first (3 µg) and second (15 µg) dose. Three piglets consistently showed elevated iNKT cell numbers and are indicated with triangle symbols. (H and I) PBMCs were isolated 7 days after the second dose (3 and 15 µg, respectively) or after a single dose of 100 µg in 2 piglets (6 weeks, 1 female and 1 male), and stained with CellTrace Violet. Cells were cultured for 4 days either in the presence of an MOMP-derived peptide (25 aa containing CD4<sup>+</sup> and CD8<sup>+</sup> epitopes) or in cell culture medium only. Proliferating cells were defined by decreased CellTrace Violet signal with the number of proliferating cells in the unstimulated condition (autoproliferation) subtracted. (J) In addition, cell culture supernatant of peptide-pulsed PBMCs was taken and analyzed for the presence of cytokines (IFN-α, IFN-γ, IL-1β, IL-10, IL-12/IL-23p40, IL-4, IL-6, IL-8, and TNF-α). Symbols represent individual data points and mean values are shown. Statistical analysis for immune cells was performed using the multiple t test with Holm-Sidak correction and Mann-Whitney for cytokines. No significant differences were found ( $p = 0.05$ ). Images created with [Biorender.com](https://www.biorender.com).

attributed this observation to the uptake of the mRNA LNP formulation by hepatocytes as no changes in liver enzymes (ALT and AST) or bilirubin were observed.<sup>18</sup> Given that the LNP composition of Galsome-NEO resembles that of marketed mRNA vaccines and considering our observation of Galsomes accumulation in the liver after i.m. injection, it is plausible that the liver vacuoles observed in this study also reflect Galsome uptake. Consistent with the BNT162b2 study, we observed unchanged bilirubin and AST levels and slightly lowered ALT levels, which are not clinically relevant unless increased. Elevated AP concentrations in rat serum might suggest liver damage; however, the absence of increased ALT or AST levels makes it unclear whether this observation is related to liver damage or other non-acute causes, such as bone resorption in response to inflammation<sup>38</sup> or bile duct obstruction. Furthermore, both histological analysis and AP normalized within 3 weeks after the final dose. Finally, it is noteworthy that previous studies have shown that intravenous administration of 2 µg of unformulated α-GC or α-GC-loaded dendritic cells induces liver damage in mice, including liver necrosis, widened intercellular space, and increased ALT.<sup>39</sup> Since we did not observe any of these phenomena and only administered a much lower dose of α-GC (90 ng) locally rather than systemically, we do not attribute liver vacuolation or elevated AP levels to α-GC. No disturbances in liver enzymes were observed in pigs.

Hematology blood analysis revealed significant changes in thrombocyte count in rats and reticulocyte count in pigs, which were considered secondary effects related to inflammation. In rats, the thrombocyte count was notably reduced, and there was an increased prothrombin time, indicating disturbed blood clotting. These changes were temporary with both, thrombocyte counts and coagulation parameters, normalizing within 3 weeks after the final dose. Despite this, it should be noted that changes in coagulation are acute side effects that should be closely monitored. In pigs, reticulocyte counts were reduced by 35%, while no significant changes were detected in the levels of hematocrit and hemoglobin. In preclinical toxicity studies of the BNT162b2, similar observations were made regarding thrombocyte counts, which decreased by 25% compared to the 35% decrease observed with Galsome-NEO.<sup>18</sup> Consistent with the BNT162b2 data, reticulocyte counts were not significantly lowered in rats 48 h after the final dose. However, a decrease in reticulocyte count was measured in the blood of rats 3 days after the first dose of BNT162b2, suggesting that the observed reticulocyte changes in Galsome-vaccinated pigs might be caused by the same mechanisms. Similar findings were reported for Moderna's mRNA 1273 vaccine, administered i.m. at doses ranging from 9 to 150 µg in Sprague-Dawley rats.<sup>36</sup> Both platelets and red blood cells were affected by inflammation. Evidence exists that platelets may undergo pyroptosis following inflammasome activation<sup>40</sup> or aggregate with neutrophils and are subsequently internalized by neutrophils due to Toll-like receptor 7 signaling.<sup>41</sup> Interestingly, uptake of mRNA LNPs in platelets has previously been reported which could relate to our observations.<sup>42,43</sup> Another explanation could be the induction of anti-platelet antibodies as observed with AstraZeneca's COVID-

vaccine ChAdOx1 nCoV-19 in humans.<sup>44</sup> However it is important to note that, despite the observations in rats, thrombocytopenia has not been commonly associated with mRNA COVID vaccines in the large-scale human trials conducted during the COVID pandemic.<sup>45</sup> Furthermore, the production and function of red blood cells (RBCs) can be impaired by several proinflammatory cytokines (e.g., TNF-α,<sup>46,47</sup> IFN-γ,<sup>48</sup> and IL-6<sup>49</sup>). In our study, IL-6 was significantly elevated with a trend toward higher IFN-γ concentrations, which could contribute to the observed hematologic changes.

We also evaluated iNKT cell responses and found increased numbers of iNKT cells in the lymph nodes of rats as well as in the whole blood of pigs. Unfortunately, we could not evaluate iNKT cell responses to the 100 µg dose in piglets, as the piglets had to be euthanized 48 h after the final vaccine dose to evaluate acute toxicity. In rats, we detected increased iNKT cell numbers in the lymph nodes but a reduced fraction of iNKT cells in the spleen, 48 h after Galsome injection. This reduction might be due to temporary downregulation of surface receptors by iNKT cells upon stimulation, as previously described,<sup>50</sup> or their migration to other tissues, such as the liver or periphery. Additionally, increased IFN-γ secretion shortly after the second and third vaccinations was observed, which suggests iNKT cell activation.

In parallel, we also assessed the potential of Galsomes to elicit T cell responses. However, since the study design was primarily focused on toxicity rather than immune activation, T cells could not be evaluated in rats due to the use of patient-specific epitope-encoding mRNA. In pigs, antigen-specific T cell responses were evaluated after two doses of 3 and 15 µg, respectively, of MOMP-encoding Galsomes. We observed proliferating CD8<sup>+</sup> (most pronounced), CD4<sup>+</sup>, and CD8<sup>+</sup>/CD4<sup>+</sup> T cells along with elevated cytokine levels (IFN-γ, TNF-α, IL-6, IL-12, and IL-10) in the supernatant of restimulated PBMCs. Interestingly, these cytokines were also found to be upregulated in the supernatant of human PBMCs upon immunization against CTH522/CAF01, a recombinant MOMP-antigen adjuvanted with a cationic liposome.<sup>51</sup> It is worth noting that the primary focus of the study was on toxicity, and since the animals were sacrificed 48 h after the final dose, the final vaccine dose might have further boosted T cell proliferation. We observed strong T cell responses in two pigs that received a single dose of 100 µg Galsome-MOMP in a preliminary experiment conducted prior to the preclinical toxicity test (referred to as “extra study” in Figure 7I).

In conclusion, our findings identified an inflammatory response in rats that received three successive doses of 30 µg Galsome-NEO-formulated mRNA. This response was characterized by cytokine secretion and an acute phase reaction, manifesting as weight loss, elevated body temperatures, and localized inflammation at the injection site. These symptoms were within the tolerated range and resolved within a few days. The observed side effects were temporary, resolving largely within 3 weeks, and were consistent with those reported in the preclinical toxicity studies for the widely used BNT162b2 and mRNA-1273 vaccines. More specifically, we

observed decreased platelet counts, hepatocyte vacuolation, and immune infiltration at the injection site in rats. In pigs, side effects were minimal besides a reduction in reticulocyte counts. As a secondary outcome, we observed the activation of iNKT cells and antigen-specific T cells in pigs. However, the study design prioritized toxicity assessment, limiting the opportunity for comprehensive immune readouts.

## MATERIALS AND METHODS

### Animals

Toxicity was evaluated in two animal species, namely Wistar Han rats and domestic piglets. The treatment of animals followed Belgian and European laws regarding animal welfare and ethics, and the study was approved by the Ethical Committee of the Faculty of Medicine and Health Sciences at Ghent University (EC 22–29) and of the Faculties of Veterinary Medicine and Bioscience Engineering at Ghent University (EC 2023/05), respectively.

Sixteen male and 16 female Wistar Han rats (age 9 weeks) were supplied by Envigo RMS B.V. (Venlo, the Netherlands) and were acclimatized for 7 days. Animals were housed in groups of the same sex in type IV cages and were offered ad libitum water and food with a rodent pellet diet (Carfill Quality, Oud-Turnhout, Belgium).

Six male and 6 female F1 hybrid (Landrace line 12 x Large White line 36) piglets (age 6 weeks) were supplied by RA-SE Genetics (Ooigem, Belgium) and were acclimatized for 7 days. In a separate study, one male and one female F1 hybrid (Landrace line 12 x Large White line 36) piglet (age 5 weeks) were supplied by RA-SE Genetics (Ooigem, Belgium) and acclimatized for 7 days. Animals were housed together in a pig stable (8 × 2.5 m) and were offered water and food (Piggistart Opti, Aveve, Leuven, Belgium) ad libitum. The stable was enriched with straw, cotton towels, metal chains, and a variety of rotating toys.

### mRNA LNP production

mRNA and mRNA LNPs were produced by the GMP unit at the Ghent University Hospital. TMG<sup>NEO</sup> mRNA was produced as previously described<sup>11</sup> and was additionally provided with Cap 1 and 1mψ. Similarly, *C. trachomatis* MOMP coding regions were inserted in the plasmid vector used for production of TMG<sup>NEO</sup>, and mRNA was subsequently prepared in a similar manner as TMG<sup>NEO</sup> mRNA. LNPs were formulated by rapid mixing of an aqueous phase containing mRNA dissolved in a 25 mM sodium acetate buffer at pH 4 and an ethanol phase containing lipids dissolved at a total concentration of 10 mM. Lipids comprised the ionizable lipidoid C12-200 (CordenPharma, Plankstadt, Germany) and helper lipids distearoylphosphatidylcholine, cholesterol, 1,2-dimyristoyl-rac-glycero-3-methoxy polyethylene glycol-2000 (Avanti Polar Lipids, Birmingham, AL, USA), and α-GC (synthesized in house by Prof. Serge Van Calenbergh as previously described<sup>52</sup>) at 50/10/38.5/1.5/0.01 mol%, respectively. The two phases were prepared at an aqueous:ethanol volume ratio of 3:1, and RNA and lipids were combined at a C12-200:RNA weight ratio of 20:1. Both phases were loaded into a syringe

(BD) and inserted in the NxGen microfluidic cartridge for mixing using a NanoAssemblr Ignite instrument (Precision Nano-systems). Microfluidic mixing was performed at a total flow rate of 12 mL/min and a flow rate ratio of 3:1 RNA:lipid. The waste volumes were 1 and 0.05 mL at the start and the end, respectively. The resulting mRNA LNP suspension was then diluted, diafiltrated, and concentrated using Tangential Flow Filtration against Tris HCl 20 mM (Avantor) 9% sucrose (Fisher Scientific) at pH 7.4. mRNA LNPs were diluted in 9% sucrose 20 mM Tris HCl buffer at pH 7.4 to yield an mRNA LNP suspension with a final concentration of 100 µg/mL mRNA, and mRNA LNPs were stored frozen in cryovials at –80°C. After thawing, batches were tested for several quality attributes, including particle size, zeta potential, mRNA encapsulation, lipid composition, and sterility. Physicochemical characteristics of the lipid formulations are shown in Table S3. Galsomes were produced according to GMP standards. Hereafter, α-GC mRNA LNPs containing TMG<sup>NEO</sup> mRNA are termed Galsome-NEO, and α-GC mRNA LNPs containing MOMP mRNA are termed Galsome-MOMP.

### Study design

Sixteen female (F) and 16 male (M) 10-week-old Wistar-Han rats were used in the preclinical toxicity study. Animals were randomly allocated to the cytokine cohort (6F/6M) or to the clinical cohort (10F/10M) (Figure 1A). Both cohorts received three repeated doses i.m. of either 30 µg patient neo-epitope (TMG<sup>NEO</sup>) mRNA encapsulated in Galsomes (Galsome-NEO rats) or an equal volume of 9% sucrose, Tris 20 mM buffer (control rats) (randomly allocated). An interval of 2 weeks was set between two doses. In the clinical cohort, clinical parameters (local reactions, temperature, and weight) were assessed on a regular basis. Forty-eight hours after the last dose, 12 rats (6M, 6F) were sacrificed to collect blood and organs for further analysis (main group). The remaining 4M and 4F rats were sacrificed 3 weeks after the last dose (recovery group), and blood and organs were again collected for further analysis. The cytokine cohort served for blood collection (on lithium heparin) 6 h after each injection to assess cytokine secretion in blood.

Six M and 6F 7-week-old piglets were randomly allocated to the control or Galsome-MOMP group and received i.m. three doses of either 3, 15, or 100 µg Galsome-MOMP (Galsome-MOMP pigs) or an equal volume of 9% sucrose Tris 20 mM buffer (control pigs) (Figure 1B). An interval of 7 days was set between two doses. Cytokine analysis and evaluation of clinical parameters were assessed in the same piglets (main group). Clinical parameters (local reactions, temperature, and weight) were assessed regularly. Blood was collected in serum tubes 5 h after each dose and used for cytokine analysis. Five hours after the third dose, additional blood was collected in heparin tubes, and PBMCs were isolated and restimulated with an MOMP peptide of 25 aa including CD8<sup>+</sup> and CD4<sup>+</sup> T cell epitopes to assess antigen-specific T cell proliferation. Four days after the first and the second dose, blood was collected in heparin tubes for iNKT analysis. 48 h after the last dose, all piglets were sacrificed to collect blood and organs for further analysis.

### Injections

Rats received i.m. injections in the right and left musculus biceps femoris with both sides receiving 150  $\mu$ L of either Tris 20 mM 9% sucrose or Galsome-NEO (i.e., 15  $\mu$ g TMG<sup>NEO</sup> mRNA at each side, corresponding to a total dose of 30  $\mu$ g TMG<sup>NEO</sup> mRNA), depending on the treatment group to which they were allocated to. During injection, rats were anesthetized in an anesthesia chamber with 5% isoflurane in oxygen and subsequently maintained with 1.5% isoflurane mixed with medical oxygen. Just before the injection, the fur at the injection sites was cut with a clipper to allow evaluation of local reactions at the injection site. Pigs were i.m. injected in the caudal region of the left musculus longissimus dorsi with volumes (30, 150, and 1,000  $\mu$ L) of either Tris 20 mM 9% sucrose or Galsome-MOMP (i.e., 3, 15, and 100  $\mu$ g MOMP mRNA). To allow measurement of body temperature, pigs were injected with a thermal microchip (BioThermo Lifechip, Destron Fearing, TX, USA) that was implanted in the area of the right hind leg by means of a subcutaneous injection 3 days before the start of the treatment.

### Assessment of clinical health status

Animals were monitored for body temperature, body weight, local reactions at the injection site, and general condition to assess their health status. In rats, the temperature was measured by inserting a rectal thermal probe (BIO-BRET2 with BIO-TK8851 thermometer, BiosebLab, Vitrolles, France). In pigs, this was done by scanning the thermal microchip (Allflex AFX-110 Reader). Local reactions at the injection (erythema, edema, and induration) were scored using the Draize scoring system as reported previously.<sup>18</sup> Representative images of the different grades of local reactions are illustrated in [Figures S1](#) and [S2](#). Weight was assessed prior to vaccination and monitored daily thereafter. All assessments were conducted at standardized time intervals, either 4 h or 24 h post vaccination and every other day thereafter.

### Blood sampling and euthanasia

During the study, blood was drawn from the tail vein in rats using a 26G IV catheter (Terumo Versatus) and was collected in heparin-coated tubes (Microvette 500 Lithium heparin, Sarstedt). In pigs, blood was drawn from the jugular vein using a 21G PrecisionGlide Needle (BD Vacutainer) and was collected in heparin-coated tubes (BD Vacutainer Lithium Heparin Tube) and serum tubes (VACUETTE TUBE CAT Serum Separator Clot Activator).

At the end of the study, blood was collected from the vena cava in rats using a Surfash Polyurethane IV Catheter 24G (Terumo) under anesthesia (5% induction and 1.5% maintenance, mixed with medical oxygen at max. 0.5 L/min) followed by exsanguination. Pigs were first anesthetized by i.m. injection of a mixture of Zoletil 100 (50 mg/mL tiletamine, 50 mg/mL zolazepam) and XylM 2% (xylazine 20 mg/mL) at a dose of 10 mg/kg. Blood was collected by percutaneous cardiac puncture followed by an intracardial injection of an overdose of sodium pentobarbital (Euthanimal 40% (400 mg/mL, at a dose of 100 mg/kg). For both animal species, blood

was collected in serum (VACUETTE), EDTA (VACUETTE), and citrate tubes (VACUETTE).

### Blood analysis

During the study, blood was collected to measure cytokine levels shortly after injection. Rat whole blood was collected in lithium heparin-coated tubes, centrifuged at 14,000 rpm for 5 min to separate plasma. Pig whole blood was collected in serum tubes, centrifuged at 1000g for 10 min to separate serum. Plasma (rats) and serum (pigs) were frozen and stored at  $-20^{\circ}\text{C}$  until analysis. In rats, cytokines (TNF- $\alpha$ , IL-10, IFN- $\gamma$ , CXCL1, MCP-1, GM-CSF, IL-18, IL-12p70, IL-1 $\beta$ , IL-17A, IL-33, IL-1 $\alpha$ , and IL-6) were measured using a bead-based multiplex assay (LEGENDplex Rat Inflammation Panel (13-plex) BioLegend, San Diego, CA, US). In pigs, cytokines (IFN- $\alpha$ , IFN- $\gamma$ , IL-1 $\beta$ , IL-10, IL-12/IL-23p40, IL-4, IL-6, IL-8, and TNF- $\alpha$ ) were measured in serum using a multiplex assay (ProcartaPlex Porcine Cytokine & Chemokine Panel 9plex, Invitrogen, Vienna, Austria). In addition, IFN- $\gamma$  was measured using an ELISA kit (Porcine IFN-gamma DuoSet ELISA, Bio-Techne).

Terminally collected blood was analyzed for biochemistry, hematology, and coagulation by a clinical laboratory (A.M.L. BV, accreditation number 8-11653-43-998, Antwerp). In rats, acute phase proteins in serum were measured by ELISA for detection of A2M and A1AGP (ab157729 and ab157730, respectively), and the assay was performed by A.M.L. BV. In pigs, serum CRP was measured in our lab using an ELISA kit (ab205089).

### Ex vivo T cell proliferation assay of porcine PBMCs

Blood collected in heparin tubes was added to Lymphoprep (STEMCELL Technologies, Vancouver, Canada) to isolate PBMCs via density gradient centrifugation. After RBC lysis in ammonium chloride, PBMCs were stained using CellTrace Violet (Invitrogen, C34571) for 20 min at room temperature (RT), washed, and resuspended in lymphocyte medium (RPMI-1640 [Gibco] supplemented with 5% heat-inactivated fetal calf serum [Gibco], 1% L-glutamine [SAFC], 1% sodium pyruvate [Gibco], 1% kanamycin [Sigma-Aldrich], 1% penicillin-streptomycin [Gibco], 1% non-essential amino acids [Gibco], and 0.1%  $\beta$ -mercaptoethanol [Merck]). Cells were seeded in a 96-well plate at a density of  $5 \times 10^5$  cells/well. Per sample, three conditions were cultured: an unstimulated condition (lymphocyte medium only), in presence of 0.5  $\mu$ g Concanavalin A (Sigma-Aldrich) or in presence of 5  $\mu$ g MOMP peptide (25 aa including CD4<sup>+</sup> and CD8<sup>+</sup> T cell epitopes, Pepsan). Cells were incubated for 96 h, and supernatant was collected and stored for further cytokine analysis at  $-20^{\circ}\text{C}$ . Next, stimulation of PBMCs was stopped by incubating PBMCs with 20 mM EDTA-PBS for 20 min at RT, and cells were subsequently collected for flow cytometry staining. Cells were stained with a fixable viability dye 1:1,000 for 30 min at  $4^{\circ}\text{C}$  (ZombieNIR, BioLegend, 423105). Next, Fc receptors were blocked by incubation in 10% pig serum for 20 min at  $4^{\circ}\text{C}$ . Cells were then surface stained by incubation of cells with 1  $\mu$ g PerCP-Cy5.5 Mouse Anti-Pig CD4a (BD, 561474), 1  $\mu$ g PE Mouse Anti-Pig CD8a (BD, 559584), and 1  $\mu$ g FITC anti-CD3 antibody (Invitrogen,

MA5-41029) during 30 min at 4°C. All samples were measured by a MACSQuant 16 flow cytometer (Miltenyi Biotec, Cologne, Germany) and analyzed by FlowJo software (BD Biosciences, Franklin Lakes, NY, USA).

### iNKT cell staining

At the day of euthanasia, half of the rat spleen and one inguinal lymph node were collected and stored on MACS Tissue Storage Solution (Cat# 130-100-008, Miltenyi Biotec). Spleens were gently pushed through a 40-µm cell strainer. After single-cell suspensions were obtained, an RBC lysis step was performed using ACK lysing buffer (Gibco, Grand Island, NY). Lymph nodes were digested with Liberase (Roche) and DNaseI (Roche) for 20 min at 37°C and subsequently filtered through a 40 µm filter cap. Single-cell suspensions were stained with a fixable viability dye 1:1,000 for 20 min at RT (LIVE/DEAD Fixable Aqua Dead Cell Stain Kit, Thermo Scientific) to exclude dead cells from analysis and subsequently incubated with Fc block 1:200 for 10 min at 4°C (anti-rat CD32, BD Pharmingen) to block nonspecific FcR binding. Subsequently, cells were surface stained with CD3-APC (1:20, REA223, Miltenyi Biotec), CD161-FITC (1:100, 3.2.3, BioLegend), and CD279-BV436 (1:100, J43, Invitrogen) during 30 min at 4°C. Compensation for spectral overlap was calculated using UltraComp eBeads compensation beads (Thermo Scientific) and MACS Comp Beads anti-REA (Miltenyi Biotec) stained with individual fluorochrome-conjugated antibodies.

At set time points, porcine whole blood was collected in lithium heparin-coated tubes and analyzed for the presence of iNKT cells. Blood was 1:10 diluted in ACK lysing buffer (Gibco, Grand Island, NY) and incubated for 10 min under gentle mixing at RT to allow RBC lysis. The cell suspension was then stained with a fixable viability dye 1:1,000 for 20 min at RT (LIVE/DEAD Fixable Aqua Dead Cell Stain Kit, Thermo Scientific). Next, Fc receptors were blocked by incubation in 10% mouse serum (Invitrogen, Catalog # 10410) for 20 min at 4°C. Cells were surface stained with mouse CD1d PBS-57 PE-labeled tetramer (1:100) and unloaded tetramer for 30 min at 4°C. Finally, an antibody staining was performed by incubation of cells with CD3ε-APC (1:50, PPT3, Southern Biotech) during 30 min at 4°C. All samples were measured by a MACSQuant 16 flow cytometer and analyzed using FlowJo software.

### Necropsy and histology

After sacrifice, a gross macroscopic evaluation was performed, and a selection of organs was weighed (lungs, liver, heart, spleen, lymph node, kidneys, and testes). Samples of tissues (liver, lungs, heart, spleen, lymph node, and injection site) were collected in a random manner and fixed in neutral-buffered formaldehyde (3.5% formaldehyde buffered with sodium phosphate) for at least 24 h. All formaldehyde-fixed tissues underwent processing, embedding, and sectioning, followed by staining with H&E according to the laboratory standard protocols. Microscopic evaluation of organs and tissue sections was performed using an Olympus BX 61 microscope (Olympus, Belgium) by a pathologist to evaluate abnormalities, necrosis, and inflammation.

### Statistical analysis

All statistical analyses were performed using the GraphPad software Prism 8 (La Jolla, CA, USA). Information on the statistical analysis is specified in the figure captions.

### DATA AVAILABILITY

The data that support the findings of this study are available within this published article and its supplemental information files.

### ACKNOWLEDGMENTS

The authors wish to thank the NIH Tetramer Core Facility for providing the mCD1d PBS-57 tetramer; Celien Kiekens, Charlotte De Bruyne, and Ibe Van de Castele for their support with the protocol design for immunogenicity testing; and Laurenz De Bock for the design of patient neo-epitope (TMG<sup>NEO</sup>) mRNA. R.V. is a postdoctoral fellow of the Research Foundation Flanders, Belgium (FWO-Vlaanderen; grant no. 1275023N), and S.M., I.A., and M.D.V. are doctoral fellows from FWO-V (grant nos. 1S73122N, 1S40923N, and 1S02723N). This research was supported by funding from FWO-V (grant nos. G040319N and G016221N), Kom op tegen Kanker (grant no. KotK\_UGent/2018/11466/L), Ghent University Concerted Research Action (BOF21/GOA/033), Ghent University Industrial Research fund (F2020/IOF-StarTT/039), and support from the Horizon Europe Project BAXERNA 2.0 (101080544).

### AUTHOR CONTRIBUTIONS

I.L., R.V., M.D., and S.M. conceptualized and supervised the project. I.L., S.C.D.S., R.V., and B.V. acquired funding. S.M., I.L., R.V., M.D., W.V.d.B., P.C., B.D., L.D.B., K.M., D.R., and D.V. contributed to the experimental design. S.V.C. and G.H. provided resources. J.I., L.D.I.M., V.R., B.C., and B.V. designed mRNA and manufactured Galsomes. S.M., I.L., R.V., M.D.V., D.R., K.M., T.E., I.A., Y.E., F.H., I.V.h., and L.D.B. contributed to the experimental work. W.V.d.B. performed histological analysis. S.M. coordinated the study and wrote the manuscript. Data analysis was performed by S.M. and R.V. I.L. and R.V. edited the manuscript. All authors reviewed and approved the submitted manuscript.

### DECLARATION OF INTERESTS

R.V., I.L., and S.C.D.S. are contributors to patent applications no. WO2020058239A1: Therapeutic nanoparticles and methods of use thereof and no. WO2023209103: Prevention and treatment of infections with intracellular bacteria, together with I.A.

### SUPPLEMENTAL INFORMATION

Supplemental information can be found online at <https://doi.org/10.1016/j.omtm.2025.101493>.

### REFERENCES

- Sung, H., Ferlay, J., Siegel, R.L., Laversanne, M., Soerjomataram, I., Jemal, A., and Bray, F. (2021). Global Cancer Statistics 2020: GLOBOCAN Estimates of Incidence and Mortality Worldwide for 36 Cancers in 185 Countries. *CA Cancer J. Clin.* 71, 209–249. <https://doi.org/10.3322/CAAC.21660>.
- Lahiri, A., Maji, A., Potdar, P.D., Singh, N., Parikh, P., Bisht, B., Mukherjee, A., and Paul, M.K. (2023). Lung cancer immunotherapy: progress, pitfalls, and promises. *Mol. Cancer* 22, 1–37. <https://doi.org/10.1186/S12943-023-01740-Y>.
- Adotévi, O., Vernerey, D., Jacoulet, P., Meurisse, A., Laheurte, C., Almotlak, H., Jacquin, M., Kaulek, V., Boullerot, L., Malfroy, M., Safety, et al. (2023). Immunogenicity, and 1-Year Efficacy of Universal Cancer Peptide-Based Vaccine in Patients with Refractory Advanced Non-Small-Cell Lung Cancer: A Phase Ib/Phase IIa De-Escalation Study. *J. Clin. Oncol.* 41, 373–384. <https://doi.org/10.1200/JCO.22.00096>.
- Besse, B., Remon, J., Felip, E., Garcia Campelo, R., Cobo, M., Masciaux, C., Madroszyk, A., Cappuzzo, F., Hilgers, W., Romano, G., et al. (2023). Randomized open-label controlled study of cancer vaccine OSE2101 versus chemotherapy in HLA-A2-positive patients with advanced non-small-cell lung cancer with resistance to immunotherapy: ATALANTE-1. *Ann. Oncol.* 34, 920–933. <https://doi.org/10.1016/j.annonc.2023.07.006>.

5. Rodriguez, P.C., Popa, X., Martínez, O., Mendoza, S., Santiesteban, E., Crespo, T., Amador, R.M., Fleytas, R., Acosta, S.C., Otero, Y., et al. (2016). A Phase III Clinical Trial of the Epidermal Growth Factor Vaccine CIMAvax-EGF as Switch Maintenance Therapy in Advanced Non-Small Cell Lung Cancer Patients. *Clin. Cancer Res.* 22, 3782–3790. <https://doi.org/10.1158/1078-0432.CCR-15-0855>.
6. Weber, J.S., Carlino, M.S., Khattak, A., Meniawy, T., Anstas, G., Taylor, M.H., Kim, K.B., McKean, M., Long, G.V., Sullivan, R.J., et al. (2024). Individualised neoantigen therapy mRNA-4157 (V940) plus pembrolizumab versus pembrolizumab monotherapy in resected melanoma (KEYNOTE-942): a randomised, phase 2b study. *Lancet* 403, 632–644. [https://doi.org/10.1016/S0140-6736\(23\)02268-7](https://doi.org/10.1016/S0140-6736(23)02268-7).
7. Rojas, L.A., Sethna, Z., Soares, K.C., Olcese, C., Pang, N., Patterson, E., Lihm, J., Ceglia, N., Guasp, P., Chu, A., et al. (2023). Personalized RNA neoantigen vaccines stimulate T cells in pancreatic cancer. *Nature* 618, 144–150. <https://doi.org/10.1038/s41586-023-06063-y>.
8. Sahin, U., Oehm, P., Derhovanessian, E., Jabulowsky, R.A., Vormehr, M., Gold, M., Maurus, D., Schwarck-Kokarakis, D., Kuhn, A.N., Omokoko, T., et al. (2020). An RNA vaccine drives immunity in checkpoint-inhibitor-treated melanoma. *Nature* 585, 107–112. <https://doi.org/10.1038/S41586-020-2537-9>.
9. Verbeke, R., Lentacker, I., Breckpot, K., Janssens, J., Van Calenbergh, S., De Smedt, S.C., and Dewitte, H. (2019). Broadening the Message: A Nanovaccine Co-loaded with Messenger RNA and  $\alpha$ -GalCer Induces Antitumor Immunity through Conventional and Natural Killer T Cells. *ACS Nano* 13, 1655–1669. <https://doi.org/10.1021/acs-nano.8b07660>.
10. Toyoda, T., Kamata, T., Tanaka, K., Ihara, F., Takami, M., Suzuki, H., Nakajima, T., Ikeuchi, T., Kawasaki, Y., Hanaoka, H., et al. (2020). Phase II study of  $\alpha$ -galactosylceramide-pulsed antigen-presenting cells in patients with advanced or recurrent non-small cell lung cancer. *J. Immunother. Cancer* 8, 316. <https://doi.org/10.1136/JITC-2019-000316>.
11. Ingels, J., De Cock, L., Mayer, R.L., Devreker, P., Weening, K., Heyns, K., Lootens, N., De Smet, S., Brussee, M., De Munter, S., et al. (2022). Small-scale manufacturing of neoantigen-encoding messenger RNA for early-phase clinical trials. *Cytherapy* 24, 213–222. <https://doi.org/10.1016/J.JCYT.2021.08.005>.
12. (2010). Corr\* Committee for Human Medicinal Products (CHMP) Guideline on repeated dose toxicity Guideline on Repeated Dose Toxicity. <https://www.ema.europa.eu/en/repeated-dose-toxicity-scientific-guideline>. CPMP/SWP/1042/99 Rev 1.
13. European Medicines Agency (2019). Guideline on quality, non-clinical and clinical requirements for investigational advanced therapy medicinal products in clinical trials. <https://www.ema.europa.eu/en/guideline-quality-non-clinical-clinical-requirements-investigational-advanced-therapy-medicinal-products-clinical-trials-scientific-guideline>. EMA/CAT/22473/2025.
14. Monzon-Casanova, E., Paletta, D., Starick, L., Müller, I., Sant'Angelo, D.B., Pyz, E., and Herrmann, T. (2013). Direct identification of rat iNKT cells reveals remarkable similarities to human iNKT cells and a profound deficiency in LEW rats. *Eur. J. Immunol.* 43, 404–415. <https://doi.org/10.1002/EJI.201242565>.
15. Schäfer, A., Hühr, J., Schwaiger, T., Dorhoi, A., Mettenleiter, T.C., Blome, S., Schröder, C., and Blohm, U. (2019). Porcine invariant natural killer T cells: Functional profiling and dynamics in steady state and viral infections. *Front. Immunol.* 10, 433288. <https://doi.org/10.3389/fimmu.2019.01380>.
16. Renukaradhya, G.J., Manickam, C., Khatri, M., Rauf, A., Li, X., Tsuji, M., Rajashekara, G., and Dwivedi, V. (2011). Functional Invariant NKT Cells in Pig Lungs Regulate the Airway Hyperreactivity: A Potential Animal Model. *J. Clin. Immunol.* 31, 228. <https://doi.org/10.1007/S10875-010-9476-4>.
17. Artiaga, B.L., Whitener, R.L., Staples, C.R., and Driver, J.P. (2014). Adjuvant effects of therapeutic glycolipids administered to a cohort of NKT cell-diverse pigs. *Vet. Immunol. Immunopathol.* 162, 1–13. <https://doi.org/10.1016/J.VETIMM.2014.09.006>.
18. Rohde, C.M., Lindemann, C., Giovanelli, M., Sellers, R.S., Diekmann, J., Choudhary, S., Ramaiah, L., Vogel, A.B., Chervona, Y., Muik, A., et al. (2023). Toxicological Assessments of a Pandemic COVID-19 Vaccine—Demonstrating the Suitability of a Platform Approach for mRNA Vaccines. *Vaccines (Basel)* 11, 417. <https://doi.org/10.3390/vaccines11020417>.
19. (2005). Guidance for Industry Estimating the Maximum Safe Starting Dose in Initial Clinical Trials for Therapeutics in Adult Healthy Volunteers Pharmacology and Toxicology Guidance for Industry Estimating the Maximum Safe Starting Dose in Initial Clinical Trials for Therapeutics in Adult Healthy Volunteers. <https://www.fda.gov/regulatory-information/search-fda-guidance-documents/estimating-maximum-safe-starting-dose-initial-clinical-trials-therapeutics-adult-healthy-volunteers>.
20. Sorensen, N.S., Tegtmeyer, C., Andresen, L.O., Piñeiro, M., Toussaint, M.J.M., Campbell, F.M., Lampreave, F., and Heegaard, P.M.H. (2006). The porcine acute phase protein response to acute clinical and subclinical experimental infection with *Streptococcus suis*. *Vet. Immunol. Immunopathol.* 113, 157–168. <https://doi.org/10.1016/J.VETIMM.2006.04.008>.
21. Heegaard, P.M.H., Stockmarr, A., Pheiro, M., Carpintero, R., Lampreave, F., Campbell, F.M., Eckersall, P., Toussaint, M.J.M., Gruys, E., and Sorensen, N. (2011). Optimal combinations of acute phase proteins for detecting infectious disease in pigs. *Vet Res* 42, 1–13. <https://doi.org/10.1186/1297-9716-42-50>.
22. Schautteet, K., De Clercq, E., Jönsson, Y., Lagae, S., Chiers, K., Cox, E., and Vanrompuy, D. (2012). Protection of pigs against genital Chlamydia trachomatis challenge by parental or mucosal DNA immunization. *Vaccine* 30, 2869–2881. <https://doi.org/10.1016/J.VACCINE.2012.02.044>.
23. Yang, G., Artiaga, B.L., Lomelino, C.L., Jayaprakash, A.D., Sachidanandam, R., Mckenna, R., and Driver, J.P. (2019). Next Generation Sequencing of the Pig  $\alpha\beta$  TCR Repertoire Identifies the Porcine Invariant NKT Cell Receptor. *J. Immunol.* 202, 1981–1991. <https://doi.org/10.4049/JIMMUNOL.1801171>.
24. Thierry, A., Robin, A., Giraud, S., Minouflet, S., Barra, A., Bridoux, F., Hauet, T., Touchard, G., Herbelin, A., and Gombert, J.M. (2012). Identification of invariant natural killer T cells in porcine peripheral blood. *Vet. Immunol. Immunopathol.* 149, 272–279. <https://doi.org/10.1016/J.VETIMM.2012.06.023>.
25. Chapman, K., Sewell, F., Allais, L., Delongea, J.L., Donald, E., Festag, M., Kervyn, S., Ockert, D., Nogues, V., Palmer, H., et al. (2013). A global pharmaceutical company initiative: An evidence-based approach to define the upper limit of body weight loss in short term toxicity studies. *Regul. Toxicol. Pharmacol.* 67, 27–38. <https://doi.org/10.1016/J.YRTPH.2013.04.003>.
26. Conti, B., Tabarean, I., Andrei, C., and Bartfai, T. (2004). Cytokines and fever. *Front. Biosci.* 9, 1433–1449. <https://doi.org/10.2741/1341>.
27. Tahtinen, S., Tong, A.J., Himmels, P., Oh, J., Paler-Martinez, A., Kim, L., Wichner, S., Oei, Y., McCarron, M.J., Freund, E.C., et al. (2022). IL-1 and IL-1ra are key regulators of the inflammatory response to RNA vaccines. *Nat. Immunol.* 23, 532–542. <https://doi.org/10.1038/s41590-022-01160-y>.
28. Ndeupen, S., Qin, Z., Jacobsen, S., Bouteau, A., Estantouli, H., and Igyártó, B.Z. (2021). The mRNA-LNP platform's lipid nanoparticle component used in preclinical vaccine studies is highly inflammatory. *iScience* 24, 103479. <https://doi.org/10.1016/J.ISCI.2021.103479>.
29. Alameh, M.-G., and Weissman, D. (2022). Nucleoside modifications of in vitro transcribed mRNA to reduce immunogenicity and improve translation of prophylactic and therapeutic antigens. <https://doi.org/10.1016/B978-0-12-821595-1.00014-2>.
30. Jain, S., Gautam, V., and Naseem, S. (2011). Acute-phase proteins: As diagnostic tool. *J. Pharm. BioAllied Sci.* 3, 118. <https://doi.org/10.4103/0975-7406.76489>.
31. Howard, E.E., Pasiakos, S.M., Blesso, C.N., Fussell, M.A., and Rodriguez, N.R. (2020). Divergent roles of inflammation in skeletal muscle recovery from injury. *Front. Physiol.* 11, 513331. <https://doi.org/10.3389/fphys.2020.00087>.
32. Lam, K., Leung, A., Martin, A., Wood, M., Schreiner, P., Palmer, L., Daly, O., Zhao, W., McClintock, K., and Heyes, J. (2023). Unsaturated, trialkyl Ionizable lipids are versatile lipid-nanoparticle components for therapeutic and vaccine applications. *Adv. Mater.* 35, 20232209624. <https://doi.org/10.1002/ADMA.202209624>.
33. Hassett, K.J., Benenato, K.E., Jacquinet, E., Lee, A., Woods, A., Yuzhakov, O., Himansu, S., Deterling, J., Geilich, B.M., Ketova, T., et al. (2019). Optimization of Lipid Nanoparticles for Intramuscular Administration of mRNA Vaccines. *Mol. Ther. Nucleic Acids* 15, 1–11. <https://doi.org/10.1016/j.omtn.2019.01.013>.
34. Meulewaeter, S., Aernout, I., Deprez, J., Engelen, Y., De Velder, M., Franceschini, L., Breckpot, K., Van Calenbergh, S., Asselman, C., Boucher, K., et al. (2024). Alpha-galactosylceramide improves the potency of mRNA LNP vaccines against cancer and intracellular bacteria. *J. Contr. Release* 370, 379–391. <https://doi.org/10.1016/J.JCONREL.2024.04.052>.
35. Verbeke, R., Hogan, M.J., Loré, K., and Pardi, N. (2022). Innate immune mechanisms of mRNA vaccines. *Immunity* 55, 1993–2005. <https://doi.org/10.1016/j.immuni.2022.10.014>.

36. CHMP. (2021). COVID-19 Vaccine Moderna, INN-COVID-19 mRNA Vaccine (nucleoside modified). [https://www.ema.europa.eu/en/documents/assessment-report/spikevax-previously-covid-19-vaccine-moderna-epar-public-assessment-report\\_en.pdf](https://www.ema.europa.eu/en/documents/assessment-report/spikevax-previously-covid-19-vaccine-moderna-epar-public-assessment-report_en.pdf).
37. CHMP. Comirnaty, INN-tozinameran, tozinameran/riltozinameran, tozinameran/famtozinameran. [https://www.ema.europa.eu/en/documents/assessment-report/comirnaty-epar-public-assessment-report\\_en.pdf](https://www.ema.europa.eu/en/documents/assessment-report/comirnaty-epar-public-assessment-report_en.pdf).
38. Terkawi, M.A., Matsumae, G., Shimizu, T., Takahashi, D., Kadoya, K., and Iwasaki, N. (2022). Interplay between inflammation and pathological bone resorption: insights into recent mechanisms and pathways in related diseases for future perspectives. *Int. J. Mol. Sci.* 23, 1786. <https://doi.org/10.3390/IJMS23031786>.
39. Hasegawa, H., Yamashita, K., Otsubo, D., and Kakeji, Y. (2016). Liver Injury After Invariant NKT Cell Activation by Free Alpha-galactosylceramide and Alpha-galactosylceramide-loaded Dendritic Cells. *Anticancer Res.* 36, 3667–3672.
40. Su, Y., Zhang, T., and Qiao, R. (2023). Pyroptosis in platelets: Thrombocytopenia and inflammation. *J. Clin. Lab. Anal.* 37, e24852. <https://doi.org/10.1002/JCLA.24852>.
41. Koupenova, M., Vitseva, O., MacKay, C.R., Beaulieu, L.M., Benjamin, E.J., Mick, E., Kurt-Jones, E.A., Ravid, K., and Freedman, J.E. (2014). Platelet-TLR7 mediates host survival and platelet count during viral infection in the absence of platelet-dependent thrombosis. *Blood* 124, 791–802. <https://doi.org/10.1182/BLOOD-2013-11-536003>.
42. Leung, J., Strong, C., Badior, K.E., Robertson, M., Wu, X., Meledeo, M.A., Kang, E., Paul, M., Sato, Y., Harashima, H., et al. (2023). Genetically engineered transfusable platelets using mRNA lipid nanoparticles. *Sci. Adv.* 9, eadi0508. <https://doi.org/10.1126/SCIADV.ADI0508>.
43. Novakowski, S., Jiang, K., Prakash, G., and Kastrop, C. (2019). Delivery of mRNA to platelets using lipid nanoparticles. *Sci. Rep.* 9, 1–11. <https://doi.org/10.1038/s41598-018-36910-2>.
44. Goh, C.Y., Teng Keat, C., Su Kien, C., and Ai Sim, G. (2022). A probable case of vaccine-induced immune thrombotic thrombocytopenia secondary to Pfizer Comirnaty COVID-19 vaccine. *J. R. Coll. Physicians Edinb.* 52, 113–116. <https://doi.org/10.1177/14782715221103660>.
45. Cines, D.B., and Greinacher, A. (2023). Vaccine-induced immune thrombotic thrombocytopenia. *Blood* 141, 1659–1665. <https://doi.org/10.1182/BLOOD.2022017696>.
46. Orsini, M., Chateauvieux, S., Rhim, J., Gaigneaux, A., Cheillan, D., Christov, C., Dicato, M., Morceau, F., and Diederich, M. (2018). Sphingolipid-mediated inflammatory signaling leading to autophagy inhibition converts erythropoiesis to myelopoiesis in human hematopoietic stem/progenitor cells. *Cell Death Differ.* 26, 1796–1812. <https://doi.org/10.1038/s41418-018-0245-x>.
47. Buck, I., Morceau, F., Cristofanon, S., Reuter, S., Dicato, M., and Diederich, M. (2009). The inhibitory effect of the proinflammatory cytokine TNFalpha on erythroid differentiation involves erythroid transcription factor modulation. *Int. J. Oncol.* 34, 853–860. [https://doi.org/10.3892/IJO\\_00000212](https://doi.org/10.3892/IJO_00000212).
48. Libregts, S.F., Gutiérrez, L., De Bruin, A.M., Wensveen, F.M., Papadopoulos, P., Van Ijcken, W., Özgür, Z., Philipsen, S., and Nolte, M.A. (2011). Chronic IFN-γ production in mice induces anemia by reducing erythrocyte life span and inhibiting erythropoiesis through an IRF-1/PU.1 axis. *Blood* 118, 2578–2588. <https://doi.org/10.1182/BLOOD-2010-10-315218>.
49. Gardenghi, S., Renaud, T.M., Meloni, A., Casu, C., Crielard, B.J., Bystrom, L.M., Greenberg-Kushnir, N., Sasu, B.J., Cooke, K.S., and Rivella, S. (2014). Distinct roles for hepcidin and interleukin-6 in the recovery from anemia in mice injected with heat-killed *Brucella abortus*. *Blood* 123, 1137–1145. <https://doi.org/10.1182/BLOOD-2013-08-521625>.
50. Wilson, M.T., Johansson, C., Olivares-Villagómez, D., Singh, A.K., Stanic, A.K., Wang, C.R., Joyce, S., Wick, M.J., and Van Kaer, L. (2003). The response of natural killer T cells to glycolipid antigens is characterized by surface receptor down-modulation and expansion. *Proc. Natl. Acad. Sci. USA* 100, 10913–10918. <https://doi.org/10.1073/pnas.1833166100>.
51. Olsen, A.W., Rosenkrands, I., Jacobsen, C.S., Cheeseman, H.M., Kristiansen, M.P., Dietrich, J., Shattock, R.J., and Follmann, F. (2024). Immune signature of Chlamydia vaccine CTH522/CAF®01 translates from mouse-to-human and induces durable protection in mice. *Nat. Commun.* 15, 1–18. <https://doi.org/10.1038/s41467-024-45526-2>.
52. Plettenburg, O., Bodmer-Narkevitch, V., and Wong, C.H. (2002). Synthesis of α-galactosyl ceramide, a potent immunostimulatory agent. *J. Org. Chem.* 67, 4559–4564. <https://doi.org/10.1021/jo0201530>.